OAA Technical Memorandum ERL WPL-72

GROUND-BASED RADIOMETRIC OBSERVATIONS OF CLOUD LIQUID IN THE SIERRA NEVADA

J. B. Snider
D. C. Hogg

Wave Propagation Laboratory
Boulder, Colorado
May 1981

noaa NATIONAL OCEANIC AND ATMOSPHERIC ADMINISTRATION / Environmental Research Laboratories

NOAA Technical Memorandum ERL WPL-72

GROUND-BASED RADIOMETRIC OBSERVATIONS OF CLOUD LIQUID IN THE SIERRA NEVADA

J. B. Snider
D. C. Hogg

Wave Propagation Laboratory
Boulder, Colorado
May 1981

UNITED STATES
DEPARTMENT OF COMMERCE
Malcolm Baldrige,
Secretary

NATIONAL OCEANIC AND
ATMOSPHERIC ADMINISTRATION
James P. Walsh,
Acting Administrator

Environmental Research
Laboratories
Joseph O. Fletcher,
Acting Director

NOTICE

The Environmental Research Laboratories do not approve, recommend, or endorse any proprietary product or proprietary material mentioned in this publication. No reference shall be made to the Environmental Research Laboratories or to this publication furnished by the Environmental Research Laboratories in any advertising or sales promotion which would indicate or imply that the Environmental Research Laboratories approve, recommend, or endorse any proprietary product or proprietary material mentioned herein, or which has as its purpose an intent to cause directly or indirectly the advertised product to be used or purchased because of this Environmental Research Laboratories publication.

CONTENTS

GROUND-BASED RADIOMETRIC OBSERVATIONS OF CLOUD LIQUID IN THE SIERRA NEVADA

J.B. Snider and D.C. Hogg
NOAA/ERL/Wave Propagation Laboratory
Boulder, Colorado 80303

ABSTRACT

Ground-based, experimental observations of cloud liquid water content were made during the 1979-80 Sierra Cooperative Pilot Project in northern California. The instrument used in these experiments was a combination receiver-radiometer designed to monitor, quantitatively, cloud liquid water by simultaneously measuring the absorption of radiation from a microwave source on a COMSTAR satellite and the microwave energy emitted by the absorbing cloud. Data recorded continuously during the December 14, 1979 to March 15, 1980 field season are described. Comparison of liquid water values measured by the radiometric system and by probes aboard an aircraft flown in the vicinity of the radiometer is discussed.

1.0 INTRODUCTION

During winter 1979-80, the Wave Propagation Laboratory participated in the Sierra Cooperative Pilot Project (SCPP) being conducted by the Water and Power Resources Service, U.S. Department of Interior. The SCPP is a research program in cloud seeding for enhanced precipitation and run-off in the Sierra Nevada; the emphasis of the program is to investigate the physical basis of the precipitation process in the northern Sierra and to determine whether increases in precipitation and snow-pack can be obtained. As a part of this study the Wave Propagation Laboratory operated a ground-based microwave radiometric instrument designed to measure the amount of liquid water contained in clouds; the major objective of the WPL participation was to demonstrate and assess the ability of the microwave radiometer to measure liquid water in clouds, continuously and remotely, from the ground. The radiometric system was operated during the SCPP

field season from December 14, 1979 through March 15, 1980. Measurements were made at a site located upwind from the SCPP test area in the Sacramento Valley of California to provide data on the liquid contained in clouds moving into the test region. The instrument was installed and aligned by WPL personnel; the operation was unattended except for maintenance of recorders and computer by local project personnel.

This technical memorandum briefly describes the theory of radiometric remote sensing of water in the atmosphere and points out some limitations of the technique. Data recorded routinely during the 1979-80 season are presented and discussed. In addition, some ground-based liquid measurements are compared with *in situ* cloud-liquid measurements made by aircraft-borne probes flown in the region of the sky observed by the radiometer. Finally, some generalizations are made about the clouds observed during the 1979-80 SCPP, and recommendations to increase the usefulness of the microwave radiometer in cloud seeding research are suggested.

2.0 MEASUREMENT THEORY

The physical basis for radiometric measurement of either liquid water or water vapor in the atmosphere is absorption of an electromagnetic wave as it passes through the water medium. The magnitude of the absorption is proportional to the amount of water present, to the temperature of the water, and to the wavelength at which the radiometric observations are made. At a wavelength of 1 cm, the absorption coefficient for liquid water varies from 1.034 to 0.445 dB/km/g/m^3 for liquid temperatures from 250 to 290 K, respectively. Whereas absorption by ice is negligible in the microwave region, absorption for liquid water at temperatures below freezing is substantial. Therefore, the microwave radiometer is capable of measuring super-cooled liquid.

For uniform clouds containing liquid water droplets that are small compared to a wavelength in the microwave region, i.e., wavelengths of the order of 1 cm, so that scattering of the electromagnetic wave can be neglected, the radiometer will observe a brightness temperature, T_b, that is related to the absorption, a, by

$$T_b = (1 - e^{-a})T_L \qquad (1)$$

where T_L is the temperature of the liquid water. Since the amount of absorption depends upon the amount of liquid present, the brightness temperature can also be related to the amount of liquid present in the clouds being observed.

The accuracy of the liquid measurement depends upon the accuracy of the brightness temperature measurement and upon the accuracy with which the temperature of the liquid can be estimated. With state-of-the-art radiometric techniques using solid-state technology, the greater uncertainty is in the determination of the liquid temperature. In general, the liquid temperature must be either assumed or estimated from observations made by other sensors, e.g., rawinsonde data. A third, statistical, technique used successfully in a dual-frequency system developed in the Wave Propagation Laboratory (Guiraud et al., 1979) makes use of a history of rawinsonde data to determine mean effective temperatures for both liquid water and water vapor.

However, the radiometric system employed in the 1979-80 SCPP utilizes a somewhat different approach — a method that allows estimates of liquid temperature to be made directly from the cloud observations. This instrument was developed, in part, to provide an independent estimate of cloud liquid contents for comparison with measurements made by the dual-frequency device mentioned above (Snider et al., 1980a). The system measures not only the brightness temperatures emitted by liquid-bearing clouds but also measures, independently, the absorption experienced by an electromagnetic wave as it passes through the cloud. Absorption is determined by observing the amplitude of a microwave beacon (frequency = 28.56 GHz, wavelength = 1.05 cm) carried on board a COMSTAR communications satellite in a geosynchronous orbit; the reduction in intensity of the beacon signal as clouds pass between the satellite and the ground-based receiver provides the direct measurement of absorption. Although the system is in reality a combination receiver-radiometer, for brevity it is referred to in this report as a radiometer.

From the simultaneous observations of brightness temperature, T_b, and absorption, a, the temperature of the liquid, T_L, can be calculated from (1):

$$T_L = \frac{T_b}{1 - e^{-a}} \quad . \tag{2}$$

With the temperature of the liquid known, the temperature-dependent absorption coefficient, $\alpha(T)$ is determined from theoretical considerations (Gunn and East, 1954; Grant et al., 1957) and the amount of liquid can be readily calculated. The procedure is briefly described in the following analysis; a more detailed treatment and a complete description of the instrument is given in Snider et al. (1980b).

For a cloud with uniform liquid density, ρ (g/m^3), and liquid temperature, T (K), the total absorption, γ in dB, experienced by a wave passing through the cloud over a distance, t (km), is

$$\gamma = \alpha(T)\ \rho t \tag{3}$$

where $\alpha(T)$ is the absorption coefficient in $dB/km/g/m^3$. The liquid content per unit cross-section, W in g/m^2, along the ray path through the cloud is

$$W = \rho t\ . \tag{4}$$

Because radiometric data do not contain information on path length, it is convenient to normalize W to a 1 km path length and unit volume; W is then obtained in millimeters and represents the total liquid contained in the entire path from radiometer to satellite. The quantity W can be converted to liquid density provided the path length through the cloud is known. For example, for W = 1 mm and t = 1 km, the liquid density is 1 g/m^3.

In practice, observation of the satellite beacon signal as a liquid-bearing cloud moves through the propagation path yields the total absorption γ. The corresponding increase in brightness temperature, T_b, produced by the liquid is used in (2) with $a = \gamma/4.34$ to determine the temperature of the liquid and subsequently the absorption coefficient $\alpha(T)$. The total liquid in the path, W (mm), is then calculated from

$$W = \frac{\gamma}{\alpha(T)}\ . \tag{5}$$

3.0 LIMITATIONS AND PRECAUTIONS

The procedure just outlined is strictly correct only if the cloud liquid is uniform and the temperature estimate given by (2) is accurate. Clouds are seldom uniform and there are often cases when clouds do not completely fill the radiometer's antenna beam. However, these situations are usually readily identified because they result in an inconsistency between absorption and brightness that causes an unreasonable estimate for the liquid temperature. In the measurements to be presented in Section 4.4, questionable values caused by these effects have been removed by editing the data. In some cases, the measured absorption has been used with an absorption coefficient based upon an assumed liquid temperature.

Since the absorption of microwaves by ice is several orders of magnitude smaller than absorption by liquid water, ice does not contribute to the brightness temperature seen by the radiometer. Therefore, the radiometric technique can discriminate between ice and liquid existing in their separate states. However, if an ice particle is covered by a layer of water, the absorption is enhanced over that for a particle that is entirely liquid. While this phenomenon is similar to that causing the "bright-band" observed with radar, it should be emphasized that the increase in absorption is a much smaller effect than the increase in reflectivity responsible for the "bright-band". For example, at a wavelength of 1 cm, the increase in absorption coefficient for a water-coated ice sphere may range up to a factor of two over that for a water-droplet (Westwater, 1972); meteorological radars routinely see increases in reflectivity in the "bright-band" by factors of 8 or more. An increase in absorption caused by a melting ice particle will cause an overestimate of the total liquid; however, the magnitude of the overestimate will depend upon the distribution of liquid along the path. To first order, the overestimate will be proportional to the ratio of the apparent amount of liquid in the melting layer to the total amount of liquid contained in the entire path. In the worst case, i.e., all liquid in the melting layer, the liquid estimate should not exceed the actual amount of liquid present by more than a factor of two.

In the data presented in Section 4.4, no attempt has been made to correct the measurements for the possible presence of a melting layer.

For water drop diameters greater than about 100 μm, the absorption is not independent of drop-size distribution and the relationships (1) - (5) may no longer be valid. Accordingly, radiometric observations of cloud liquid made when rain is falling along the propagation path must be used with caution. Curves relating attenuation at 28.56 GHz to the rain rate for Laws-Parsons and Marshall-Palmer drop-size distributions are shown in Fig. 1; the curves were calculated using attenuation-rain rate relationships reported by Olsen et al. (1978). Study of Fig. 1 shows that even low rain rates of 2 or 3 mm/hr can cause absorptions comparable to or exceeding that for non-precipitating clouds which rarely have absorptions exceeding 2 dB. Therefore, rainfall extending over a large part of the propagation path may mask absorption by liquid in the cloud.

Moisture or snow (especially wet snow) on the antenna reflector (Fig. 2) may also cause measurement errors. These errors may arise in two ways: undesired steering of the antenna beam off of the propagation path to the satellite due to a layer of moisture partially covering the reflector, and the increase in brightness temperature caused by the moisture on the reflector surface. These effects cannot be distinguished from those caused by a cloud passing through the antenna beam.

Tests to evaluate the uncertainties in cloud liquid estimates caused by a wet reflector were performed by wetting the reflector using a garden tank-sprayer and observing the increases in absorption of the satellite beacon signal and brightness temperature. The measurements show that an apparent increase in absorption of 0.3 dB and an increase in brightness temperature of 18 K can result from a thin layer of water upon the parabolic antenna surface. These values correspond to an apparent cloud liquid value of 0.4 mm. Although this amount of liquid is small compared to that contained in a wet cloud, liquids measured immediately after a rain shower may be somewhat lower than indicated by the instrument.

Errors in the direct absorption measurement may result from undetected changes in the satellite's orbit. Although the position of the satellite is maintained to within 0.1 degree as viewed from the earth's surface, orbital variations within this window combined with small antenna pointing errors may result in a small but important variation in the received beacon level. Therefore, the diurnal variation

of the power received from the microwave beacon is determined during clear sky conditions to establish a reference level. However, changes in the clear sky reference level caused by a slight change in orbit made to maintain the satellite's position may go undetected during extended periods of cloud cover or precipitation. Since the absorption is measured relative to the clear-sky reference level, an unknown change in orbit could cause an error in the absorption measurement. The error in the liquid estimates caused by an unknown shift in reference level should not exceed ±0.1 mm. Of course, this error is removed when a new reference level is established with the return of clear skies.

Because of the several variables just discussed, particularly when it is raining at the site, the absolute accuracy of the liquid measurement is difficult to assess. Although it is possible to estimate uncertainties in the absorption and brightness temperature observations, unknowns such as incomplete filling of the antenna beam and the presence of melting ice particles preclude a realistic evaluation of the measurement accuracy. However, of greater importance than absolute measurement accuracy is the fact that the microwave radiometer will indicate the presence of relatively small amounts of liquid water at any temperature. Further, the instrument provides a continuous record of the liquid as it passes through the instrument's field of view.

4.0 1979-80 SCPP CLOUD OBSERVATIONS

4.1 Radiometer Location

During the 1979-80 SCPP field season, the radiometer was installed at the Sheridan, California WPRS site (39°1'N, 121°20'W). Elevation and azimuth angles of the COMSTAR satellite from Sheridan are 32.6° and 132.6°, respectively; the radiometer antenna remained fixed at these angles throughout the measurement period. Therefore, all data are for clouds drifting through a fixed propagation path. The geometry of the path relative to the SCPP test area is shown in Fig. 3; the altitude of the antenna beam is plotted versus range from the radiometer in Fig. 4. Figure 4 can be used to estimate the range from Sheridan at which clouds may be observed; for example, for cloud tops at a height of 5 km, clouds within 9 km from

the site can be observed. The antenna half-power beamwidth is 0.6 degree; the spread of the antenna beam with range is shown by the dashed lines. The elevation of the Sheridan site is 60 m, MSL.

The WPRS Skywater radar (wavelength = 5.4 cm) and a rawinsonde facility were located at the Sheridan site; standard meteorological surface observations were also made. A photograph of the Sheridan installation is shown in Fig. 2. A second 5 cm radar, operated by NCAR, was located about 10 km south of the Sheridan site.

4.2 Data Reduction and Display

Some computer hardware required for real-time processing of the data was not available until February, 1980. As a result, for the period from 14 December 1979 to 16 February 1980, liquid data were not processed in real-time. However, a strip-chart presentation of absorption and brightness temperature was displayed at the Skywater radar van to provide a qualitative indication of cloud liquid for use by the site manager and radar operator.

Real-time data processing began on 17 February 1980 using an LSI-11 mini-computer. The absorption and brightness temperature outputs from the radiometer were sampled at a 10 Hz rate and averaged for 10 seconds. Liquid values were computed from these 10 second averages. All three quantities were averaged and written onto a floppy disk at 60 second intervals. A strip-chart record of the total path liquid was displayed at the radar van; these analog liquid values were updated every 30 seconds.

4.3 Post-Experiment Data Processing

The strip-chart data (absorption and brightness) recorded from mid-December through mid-February were scaled after the experiment and converted to total path liquid. These liquid data, read at 1.5 min intervals, are plotted versus time in Figs. 5 through 20. The absorption, brightness and liquid data which had been written on floppy disk, were edited for errors and possible problems associated

with the limitations outlined above. After editing, the liquid data were recalculated and are plotted versus time in Figs. 21 through 28. The liquid plots are limited to 6 mm because higher amounts of liquid are nearly always caused by heavy rainfall.

Rainfall data, recorded at the Sheridan site using a weighing bucket rain gage with an 8-inch aperture, are plotted versus time alongside the path liquid data to aid in interpretation of the amounts of liquid. The rain rate, plotted as a vertical bar, represents the rainfall in mm that has fallen during the preceding 15 min period.

4.4 Discussion of Data

In this section, the entire data set recorded during the measurement period is reviewed. The discussion indicates some general features of the cloud liquid observed during the 1979-80 SCPP. While no rigorous attempt to classify cloud liquid by cloud type is made, the general character of the radiometer output is related to the probable cloud type to aid in interpretation of the data. These relationships are based upon past experience in Colorado over a year's time as well as the current observations in the Sierra Nevada.

Reference to Figs. 5 through 28 will be helpful in reading the following discussion.

Day 353 -- The data show an increase in liquid to about 1 mm prior to the start of precipitation. The liquid record is characteristic of strato-cumulus clouds.

Day 354 -- These data are typical of liquids observed in strato-cumulus clouds where the liquid maxima are due to imbedded dense cumulus clouds. The large amount of liquid seen near 2300 GMT may be caused by virga or rain falling along the path but not at the radiometer site.

Day 355 -- Liquid values observed until 0800 GMT are largely associated with rainfall; during most of this period, attenuation by the rain masks absorption by the cloud liquid. After 0800, most of the liquid is contained in non-precipitating clouds. However, the very narrow peaks may be due to virga or rainfall away from the radiometer site.

Days 357, 358 -- After an increase in cloud liquid to some 0.7 mm before the onset of rain, the remaining liquid data are largely due to rain. The system is shut down due to a primary power failure at 0505 GMT, day 358.

Days 4, 5, 6, 7, 8 -- These data are good examples of liquids contained in isolated, cumulus clouds. The peak liquid value of 4.5 mm occurring at 2230 GMT on day 4 is probably caused by virga. However, the lower liquid values are routinely observed in non-precipitating clouds.

Day 9 -- A general increase in cloud liquid is seen until about 1300 GMT. However, a decrease in liquid occurs from 1330 to 1600 prior to the start of rain. It is interesting to speculate on whether the decrease in liquid indicates a change from liquid to ice within the clouds. After 1600 GMT, attenuation by rain obscures the cloud liquid.

Days 10 through 18 -- During this period several storms from Pacific semi-tropical regions pass through the area. Data contain many periods of rain interspersed with both clear skies and non-precipitating clouds. In most cases, the rainfall obscures the cloud liquid. The variable nature of the radiometric data after 1200 GMT on day 11 suggests that liquid is passing through the area in bands or in convective cells.

Days 25, 26, 31 through 34, 36, 37, 42 -- This time period is characterized by mostly non-precipitating clouds with light rainfall on days 34 and 37. Cloud liquid data for day 31 appear to be for stratus with imbedded wet cumulus clouds. Stratus and cumulus clouds pass through the radiometer antenna beam at various times for the other days in this sequence.

Days 45 through 53 -- On these days a series of Pacific storms passed through the test area in a manner similar to the events of mid-January. Fairly heavy rain fell during most of this time. The plots of rain versus time clearly show those radiometer data that should not be used for estimation of cloud liquid.

Day 45 shows the general build-up of liquid preceding this series of storms; the peak value of 3.7 mm just before 0800 GMT may be due to virga. On day 46, note the decreases in liquid at 0700 GMT and 1500 GMT; in both instances, heavy rainfall occurs shortly after the decrease in liquid.

Gaps up to several hours duration appearing in the liquid data on days 48 and 49 are caused by installation of the computer and other tasks associated with the start of real-time data processing. However, these interruptions took place during periods of rain so little cloud-liquid data are lost. The brief decreases to zero liquid seen at 4 hour intervals on day 48 are caused by automatic self-calibrations by the radiometer. Actually, these calibration periods are present in all the data but are not so noticeable as on day 48. The apparent breaks in the liquid record from 0800-1630 GMT, day 50, are the result of radiometer saturation caused by the large attenuations produced by heavy rainfall.

An interesting event is the decrease in liquid observed late in day 50 and continuing through most of day 51. The relatively brief, small values of liquid seen until about 1300 GMT, day 51, are probably caused by post-frontal cumulus clouds. A general increase in cloud liquid typical of stratocumulus clouds begins at 1315 GMT followed by rain at 0000 GMT, day 52.

Day 59 -- As a result of a primary power failure at 1915 GMT, day 54, radiometer data are missing until approximately 1300 GMT, day 59. The liquid seen for the remainder of this day is contained in stratus and cumulus clouds. Significantly, the Skywater and NCAR radars (wavelength $\approx$ 5 cm) reported few echoes during this period and were shut down at 2200 GMT.

Day 62 -- This is the day of the unfortunate crash of the Desert Research Institute's B-26 cloud physics aircraft at about 1930 GMT. The radiometer observed cloud liquid of some 0.3 mm at this time while the apparent liquid temperature was below freezing. Sheridan is located approximately 40 km west of the crash location.

Day 63 -- The first known instance of radiometric data being used, at least in part, to initiate cloud seeding occurred on this day. As recorded in the daily operations log by Moore (1980), at 0745 PST (1545 GMT) the sky at Sheridan was overcast and few echoes were observed by the 5 cm radars. However, on the basis of 1.5 to 2 mm of cloud liquid being observed by the radiometer, the decision was made to launch the University of Wyoming's cloud physics aircraft (N2UW) to measure liquid in the vicinity of the propagation path. Because the aircraft measurements confirmed the presence of fairly large quantities of liquid, it was decided to perform a randomized seeding experiment. Seeding was performed in regions containing liquid water and little ice; in all cases, positive seeding signatures were found by the cloud physics aircraft (Stewart and Marwitz, 1980). Since seeding was performed downwind from the propagation path, possible seeding effects in the radiometer's output could not be observed. However, this event illustrates the potential usefulness of the microwave radiometer in locating seedable regions in liquid-bearing clouds.

Earlier this day, a decrease in cloud liquid at 0655 GMT precedes a period of heavy rain from 0730 to 0900 GMT.

Day 64 -- These data show relatively small amounts of liquid contained in post-frontal clouds.

Days 65 and 66 -- The data show the build-up and decay of liquid during a relatively brief frontal passage. Considerable convection accompanied this system with the radiometer suffering saturation at times. Some data were lost due to power failures at Sheridan. The cloud physics aircraft was struck by lightning on day 65 effectively ending its participation in the 1979-80 SCPP field season.

Day 71 -- The structure of the liquid suggests convective clouds. A computer disk change followed by a primary power failure resulted in the loss of some data.

Day 73 -- Liquid observed in cumulus clouds.

Days 74 and 75 -- The liquid was contained in non-precipitating overcast (strato cumulus) until start of rain at 2230 GMT, day 74. This is another event where the total path liquid decreased shortly before (2200 GMT) the start of rain (2215 GMT).

Data collection was terminated with the passage of the storm system from the area on day 75.

4.4.1 Climatology

The following generalizations may be made relative to the cloud liquid observed by the radiometer employing the COMSTAR beacon in 1979-80. Note that these generalizations are for an elevation angle of 32.6 degrees.

In stratus clouds, the total path liquid is generally less than 0.5 mm and rarely exceeds 0.7 mm.

Wet cumulus clouds imbedded in stratus may cause the total path liquid to increase to 1.5 mm.

Path liquids up to 1 mm are found in isolated cumulus clouds; a typical value is 0.5 mm.

Total liquids up to 5 mm or greater are observed in convective cloud systems. However, these large values are often associated with virga, which may contain relatively large dropsizes. Therefore, some of these cases should probably be considered equivalent to liquid values caused by rain rather than by non-precipitating clouds.

4.5 Comparison of Aircraft and Radiometer Liquid Measurements

One objective of the 1979-80 SCPP was to obtain independent *in situ* cloud liquid data for comparison with radiometric measurements. Although liquid observations by the radiometer employing the COMSTAR beacon had been found to agree on

the average within 10% with data from an independent radiometric system (Snider et al., 1980a), it was considered desirable to attempt additional comparisons with data from probes carried by the cloud physics aircraft (N2UW). Two types of liquid sensors are carried on the aircraft: a Johnson-Williams "hot-wire" probe (JW) and a forward scattering spectrometer probe (FSSP). The J-W probe directly measures cloud liquid water content (LWC) in g/m^3. The spectral data from the FSSP must be integrated to obtain the liquid water content; the spectral response of the FSSP is from 0.5 to 45 μm in 15 channels. Since the radiometer measures the total path liquid in mm, the two sets of data must be brought to a common point of comparison: this has been accomplished by converting the total path liquid from the radiometer to average liquid content in g/m^3. To make the conversion, the total liquid (mm) is divided by the path length through the clouds.

Unfortunately, the comparison is complicated because the aircraft and radiometer must sample different paths. Due to safety and other considerations, the aircraft could sample the liquid on a 10 degree path whereas the elevation angle of the propagation path is 32.6 degrees. Therefore, it is necessary to translate the data between the two paths. The translation requires the assumption of a uniform distribution of liquid versus height in the regions being observed by the aircraft and radiometer. Although this assumption is highly questionable, nevertheless it was decided to attempt the comparison.

A total of eight flights were made in the vicinity of the propagation path. Seven flights were made along a 10 degree elevation angle and a 132.6 degree radial from the radiometer site. During the first flight, the aircraft flew horizontal paths through clouds along the 132.6 degree radial. However, the latter procedure was abandoned because of the large amount of time required and the problem of obtaining flight clearance. During four flights, rain at the radiometer obscured liquid in the clouds so that data comparisons are meaningless. A comparison of data recorded during the remaining flights is given in Table I.

Since it is necessary to assume uniform distribution of liquid with height to place the data on a common basis for comparison, LWC data in Table I have been translated to a vertical path. Thus, table values represent the average LWC for a vertical column through the cloud. The data can be converted to average LWC

Table I.--Comparison of liquid water content measured by aircraft probes and radiometer

Date/Time(GMT)	Liquid Water Content (g/m^3) FSSP	JW	Radiometer
1/09 - 0113	.05 (0.1)	.08 (0.2)	.07
2/16 - 2226	.03 (.08)	.04 (.07)	.13
3/03 - 1636	.10 (0.4)	.14 (0.5)	.33
3/03 - 1643	.09 (0.3)	.06 (.25)	.30

along a slant path by dividing the vertical LWC by the sine of the path elevation angle. The path length used to convert the radiometer total liquid values to LWC was estimated from the aircraft data, from RAWIN-sonde data when recorded near flight time, and from pilot reports. The values in parentheses are the maximum LWC's observed by probes on the aircraft during the flight.

The agreement between radiometer and aircraft data varies from excellent to differences of a factor of 4 or 5. In general, the comparison may be no better or worse than could be expected considering the differences in technique and sample path, the required assumptions and the difficulty of the measurement. (For example, simultaneous liquid measurements by the two types of aircraft probes sometimes differ by a factor of two or more.) However, the tendency for the radiometer to indicate greater liquid than the airborne probes is believed to be caused by liquid existing below the 3000 feet minimum obstacle clearance altitude (MOCA) and not being observed by the aircraft. This was almost certainly the case on 16 February when the author observed liquid bearing clouds below 3000 feet at the time of the aircraft flight.

5.0 CONCLUSIONS AND RECOMMENDATIONS

The experience acquired during the 1979-80 SCPP field season has shown the effectiveness of microwave radiometric techniques in observation of liquid water in clouds. It has been shown that radiometric technique is a useful complement to

other techniques such as radar and aircraft-borne cloud probes. For example, the events of 3 March 1980 show that radiometric data, appropriately combined with data from other sensors, may ultimately be capable of identifying seedable regions in clouds containing liquid in the form of very small drops.

On several occasions during the field season, total path liquid was observed to decrease shortly before the start of rainfall. One interpretation of this phenomenon is that the radiometer is observing a change of phase from liquid to ice preceding the precipitation. If this is indeed the case, it may be possible for a radiometer with a steerable antenna beam to monitor the effects of seeding in clouds. On the other hand, a number of cases were also observed where rain began while the total path liquid was increasing. Thus, evaluation of the radiometer's ability to detect changes of phase reliably must await further experimentation.

Comparison of *in situ* cloud liquid measurements by aircraft-borne probes with radiometric data produced mixed results. Some of the differences are probably due to measurement technique and the inability of aircraft and radiometers to sample liquid along identical paths. However, the comparison does seem to indicate that the aircraft does not observe substantial amounts of liquid located below the 3000 feet minimum obstacle clearance altitude.

The lack of range information, inherent in radiometric observations of the atmosphere, may be alleviated by combining radiometric and radar data. However, to insure detection of clouds with low liquid content and to obtain compatibility with the radiometric data, the radar should operate at millimeter wavelengths. In addition, the radar should have the ability to measure backscattered energy on orthogonal polarizations in order to discriminate between liquid and ice. Data provided by these two systems operating in tandem can greatly increase our knowledge of the distribution of liquid in clouds.

For maximum usefulness, future radiometric observations should be made with a steerable antenna beam to allow observation of cloud liquid in any direction. Therefore, the radiometer must be a passive system rather than a system that employs a satellite-borne beacon. Recent work has demonstrated that a two-frequency passive system can accurately measure cloud liquid including supercooled water (Hogg et al., 1980; Snider et al., 1980a).

Little is presently known about the variation of water vapor in the atmosphere and its importance in cloud seeding. Continuous observation of water vapor as well as liquid may provide new insight into this question. Therefore, it is recommended that future cloud seeding experiments employ a dual-frequency radiometer with a steerable beam that simultaneously measures both liquid water and water vapor.

6.0 ACKNOWLEDGMENTS

The work reported herein was supported by the Water and Power Resources Service, U.S. Department of the Interior. Aircraft measurements of cloud characteristics were supplied through the courtesy of Prof. J.D. Marwitz, University of Wyoming. The author wishes to thank Mr. Will Scott and other personnel of Electronic Techniques, Inc. for minding the radiometer during the field season. Rainfall data were processed by Atmospherics, Inc. and supplied to the author by WPRS. Mr. Harold Burdick of the Wave Propagation Laboratory participated in construction and implementation of the instrument, and Mr. E.E. Muller of Bell Laboratories advised on the COMSTAR satellite beacon. We thank Ms. Mildred Birchfield for her excellent typing of the manuscript.

7.0 REFERENCES

Grant, E.H., T.J. Buchanan, and H.F. Cook (1957), Dielectric behavior of water at microwave frequencies, J. Chem. Phys. 26, 156-161.

Guiraud, F.O., J. Howard, and D.C. Hogg (1979), A dual-channel microwave radiometer for measurement of precipitable water vapor and liquid, IEEE Trans. Geosci. Electron., GE 17(4), 129-136.

Gunn, K.L.S., and T.W.R. East (1954), The microwave properties of precipitation particles, Quart. J. Roy. Meteorol. Soc., 80, 522-545.

Hogg, D.C., F.O. Guiraud, and E.B. Burton (1980), Simultaneous observation of cool cloud liquid by ground-based microwave radiometry and icing of aircraft, J. Appl. Meteorol, 19(7), 893-895.

Laws, J.O., and D.A. Parsons (1943), The relation of raindrop-size to intensity, Trans. Amer. Geophys. Union (24), 452-460.

Marshall, J.S., and W. McK. Palmer (1948), The distribution of raindrops with size, J. Meteorol (5), 165-166.

Moore, J.A. (1980), private communication.

Olsen, R.L., D.V. Rogers, and D.B. Hodge (1978), The aR^b relation in the calculation of rain attenuation, IEEE Trans. Antennas Propagat. AP 26(2), 318-329.

Snider, J.B., F.O. Guiraud, and D.C. Hogg (1980a), Comparison of cloud liquid content measured by two independent ground-based systems, J. Appl. Meteorol., 19(5), 577-579.

Snider, J.B., H.M. Burdick, and D.C. Hogg (1980b), Cloud liquid measurement with a ground-based microwave instrument, Radio Sci., 15(3), 683-693.

Stewart, R.E., and J.D. Marwitz (1980), Cloud physics studies in SCPP during 1979-80, Report No. AS125, Dept. of Atmospheric Science, University of Wyoming, Laramie.

Westwater, E.R. (1972), Microwave emission from clouds, NOAA Tech. Rep., ERL 219-WPL 18.

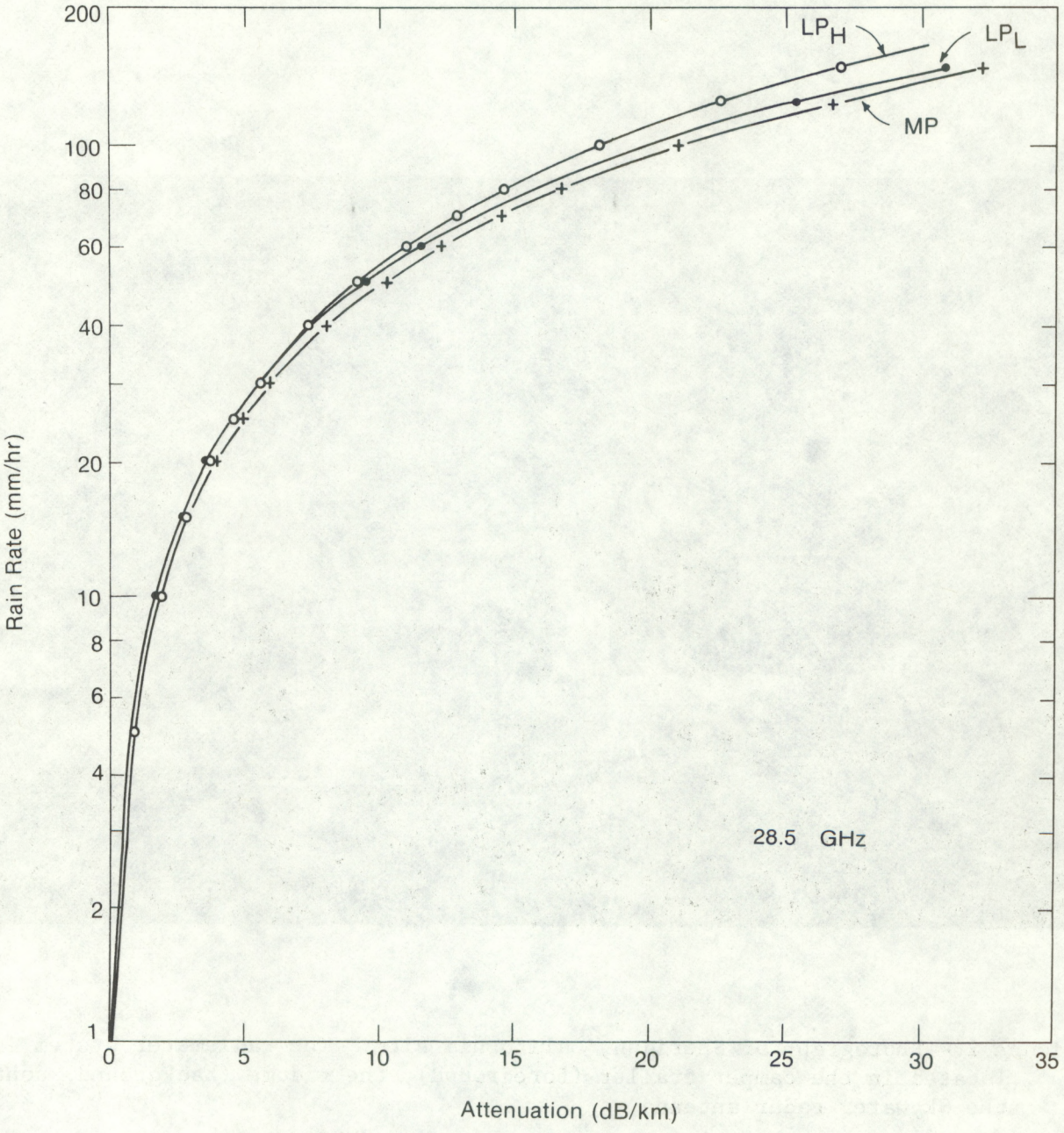

Figure 1.--Attenuation at 28 GHz vs. rain rate for Laws-Parsons (LP) and Marshall-Palmer (MP) drop-size distributions. L and H are curves obtained using low and high rain rates by Olsen et al. (1978).

Figure 2.--Photograph of Sheridan, California site. The radiometer system is located in the camper trailer (foreground); the radome (background) contains the Skywater radar antenna.

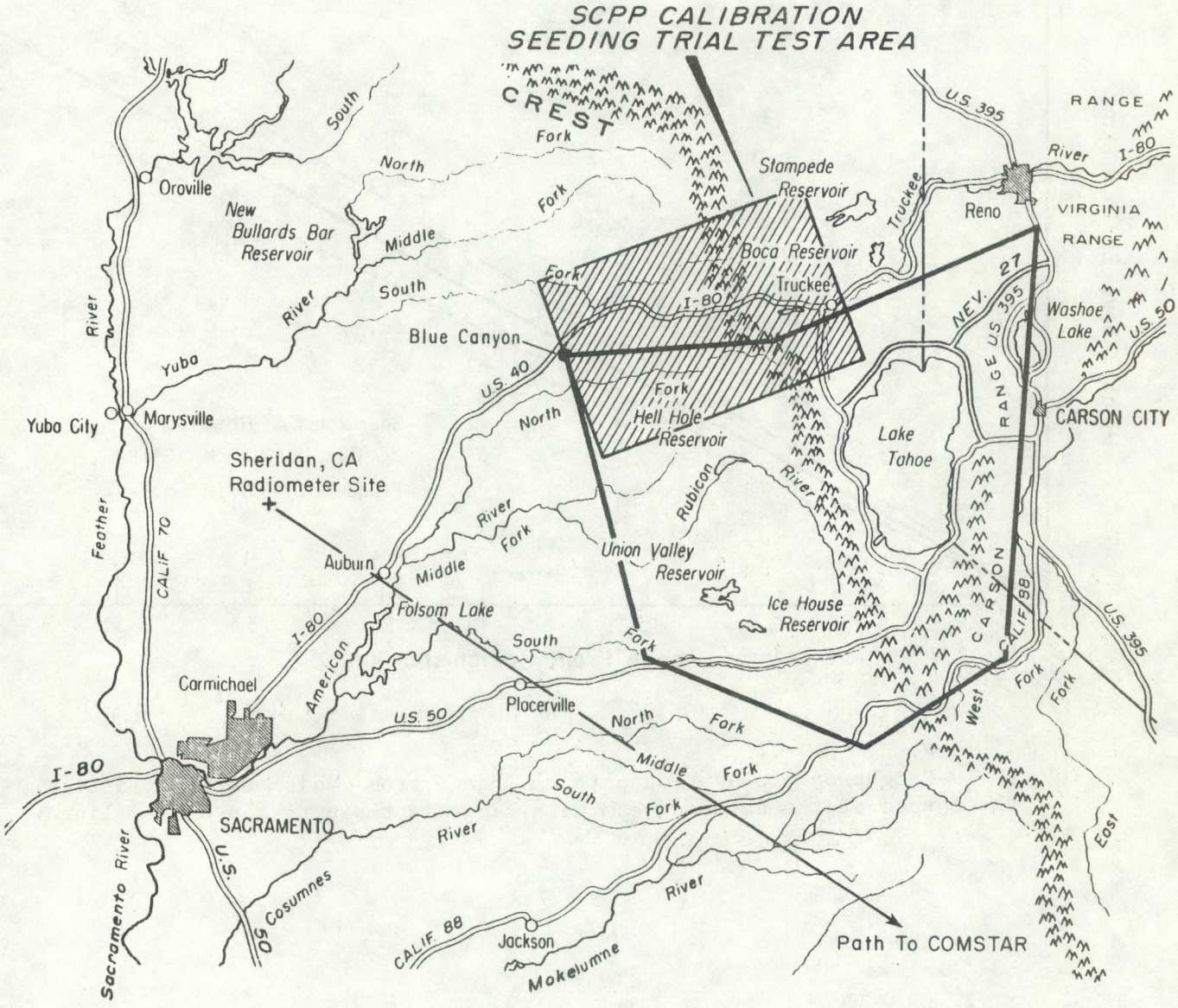

Figure 3.--Plan view showing earth-satellite propagation path relative to SCPP test area.

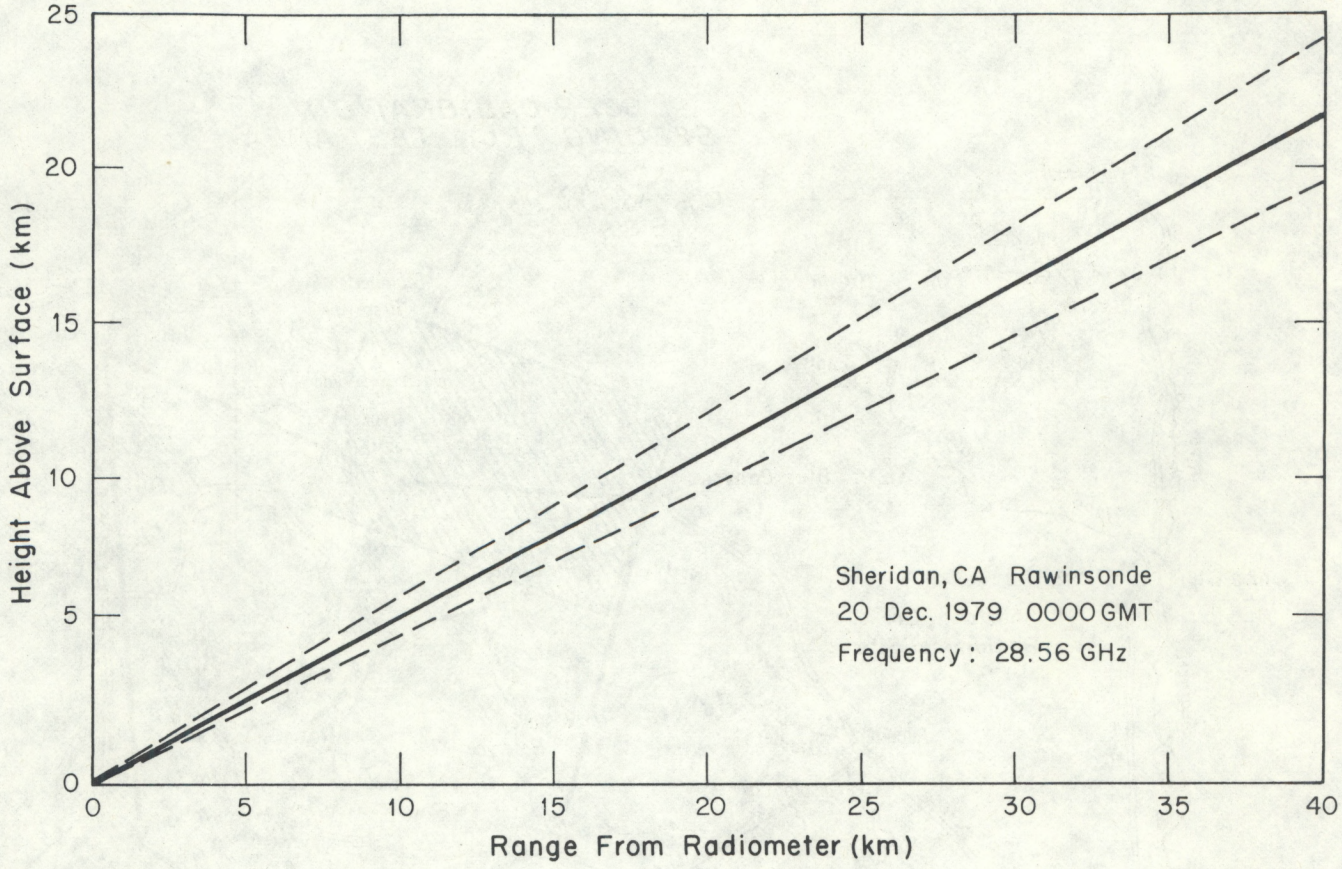

Figure 4.--Height of propagation path vs. range from radiometer (solid line); the spread of the antenna beam with range is shown by the dashed lines.

Figures 5-28.--Time series of total path liquid measured by the radiometer and rainfall measured at the Sheridan site.

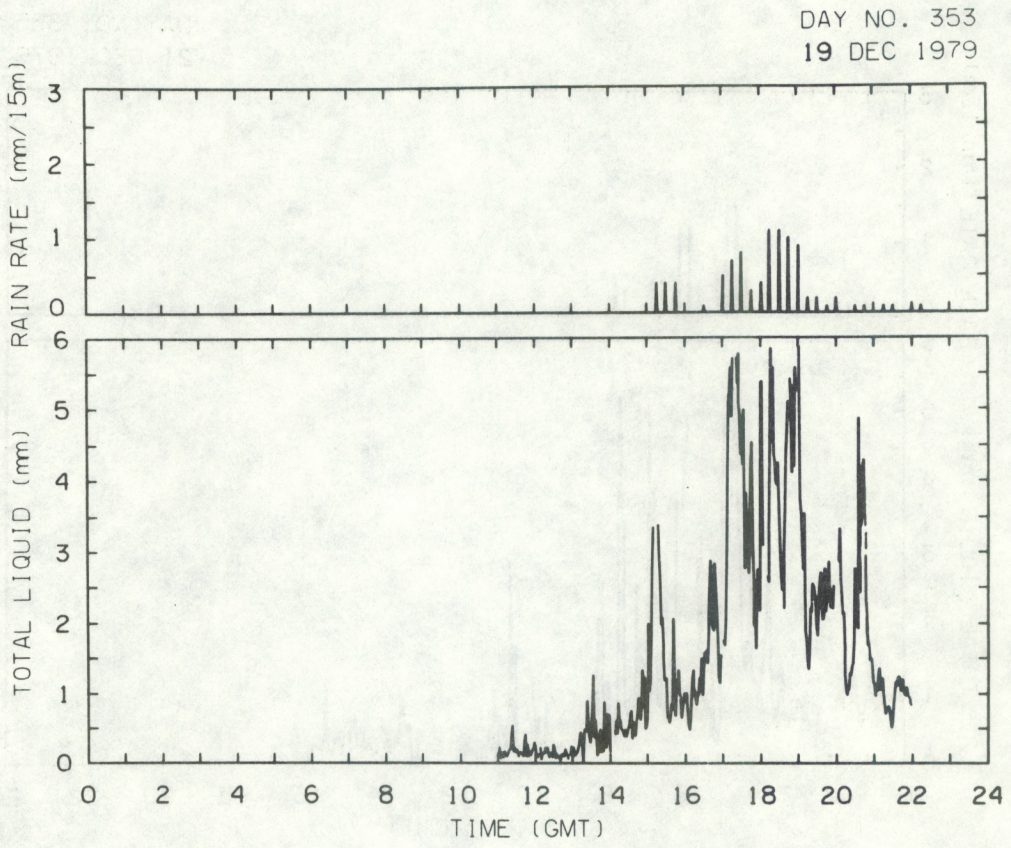
DAY NO. 353
19 DEC 1979
RAIN RATE (mm/15m)
TOTAL LIQUID (mm)
TIME (GMT)

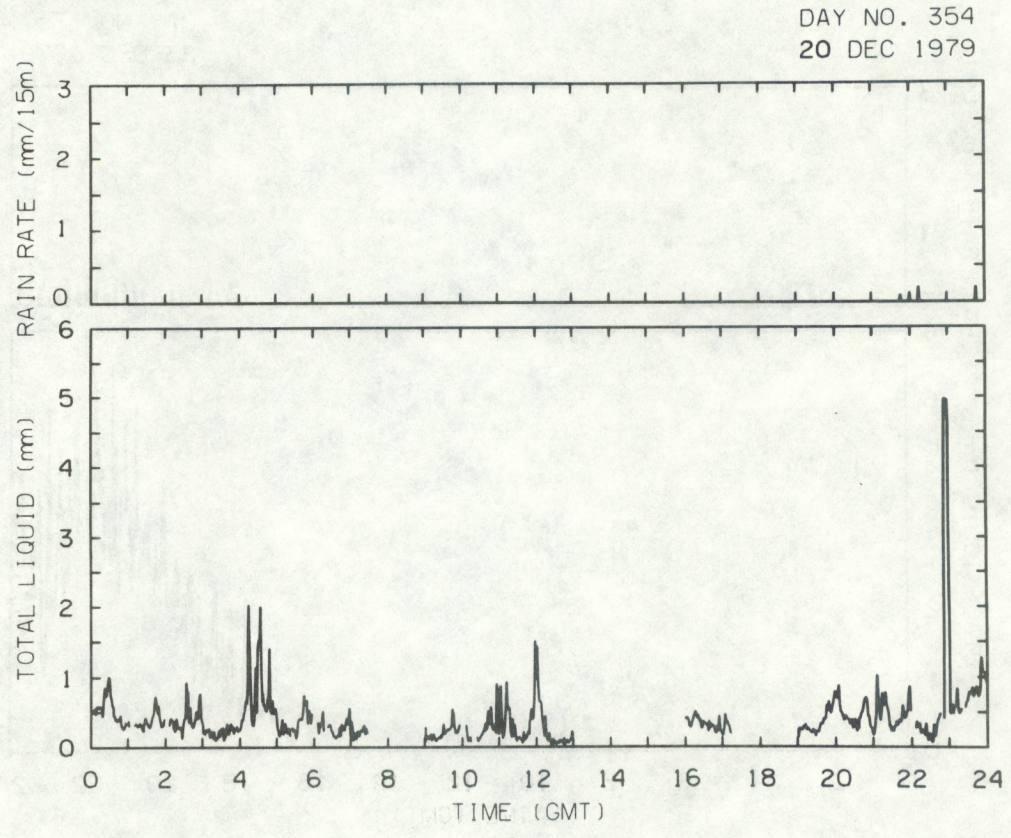
DAY NO. 354
20 DEC 1979
RAIN RATE (mm/15m)
TOTAL LIQUID (mm)
TIME (GMT)

Figure 5

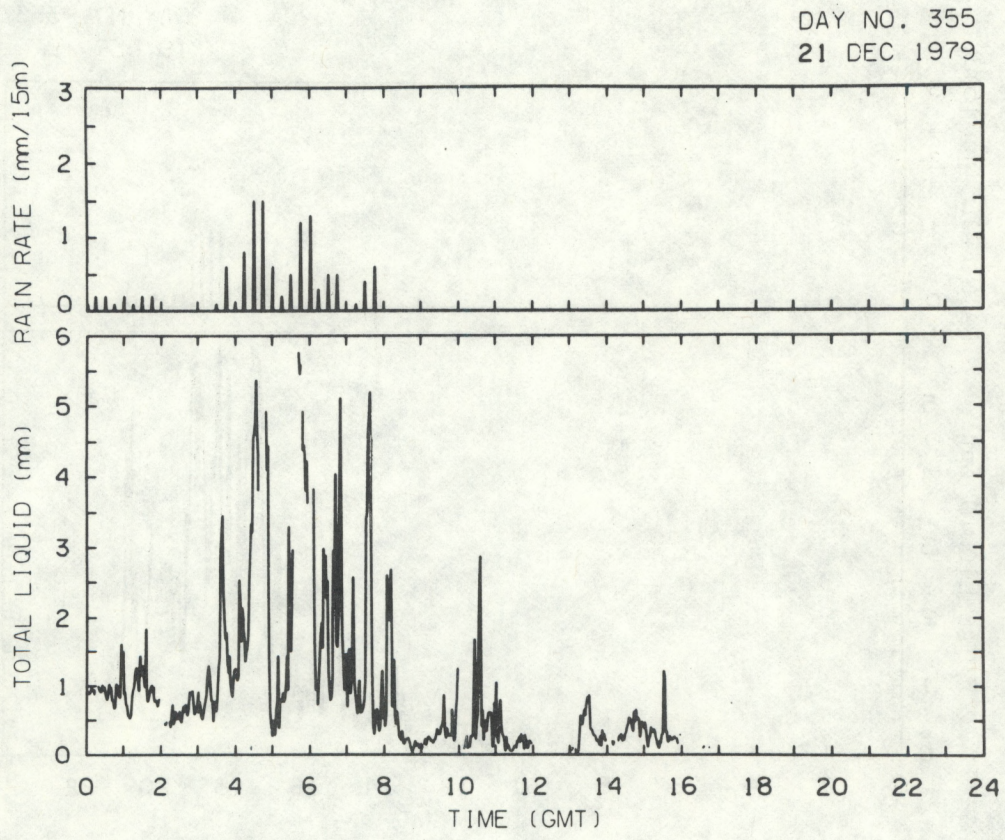
DAY NO. 355
21 DEC 1979
RAIN RATE (mm/15m)
TOTAL LIQUID (mm)
TIME (GMT)

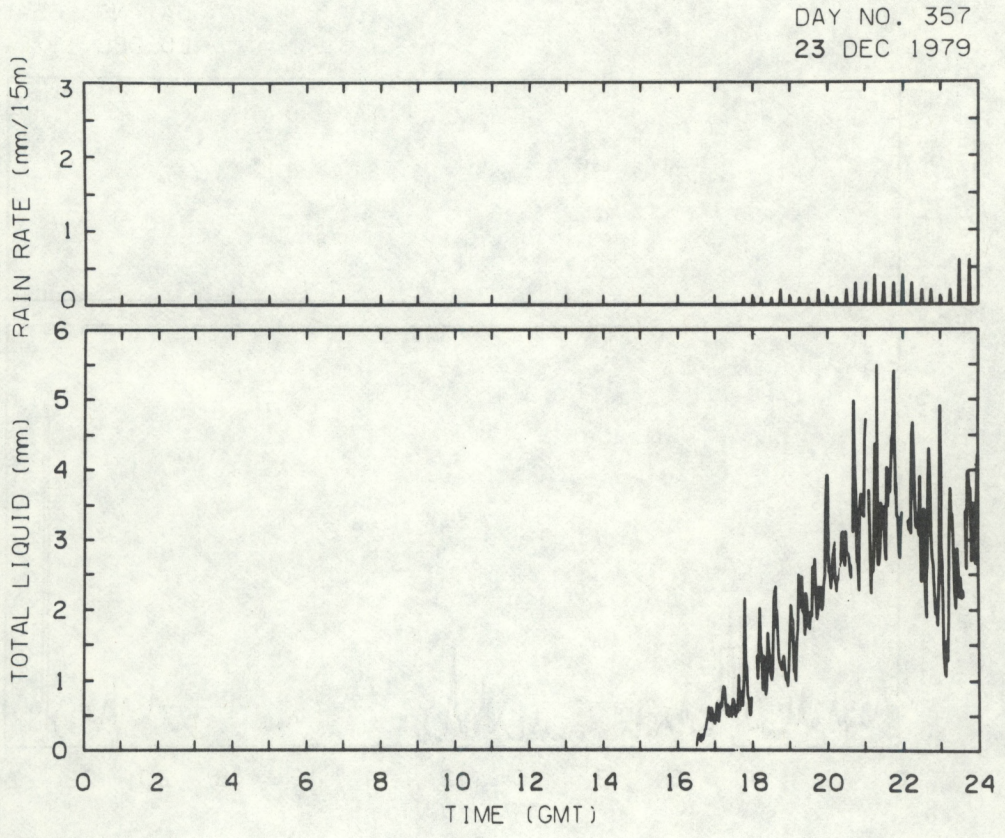
DAY NO. 357
23 DEC 1979
RAIN RATE (mm/15m)
TOTAL LIQUID (mm)
TIME (GMT)

Figure 6

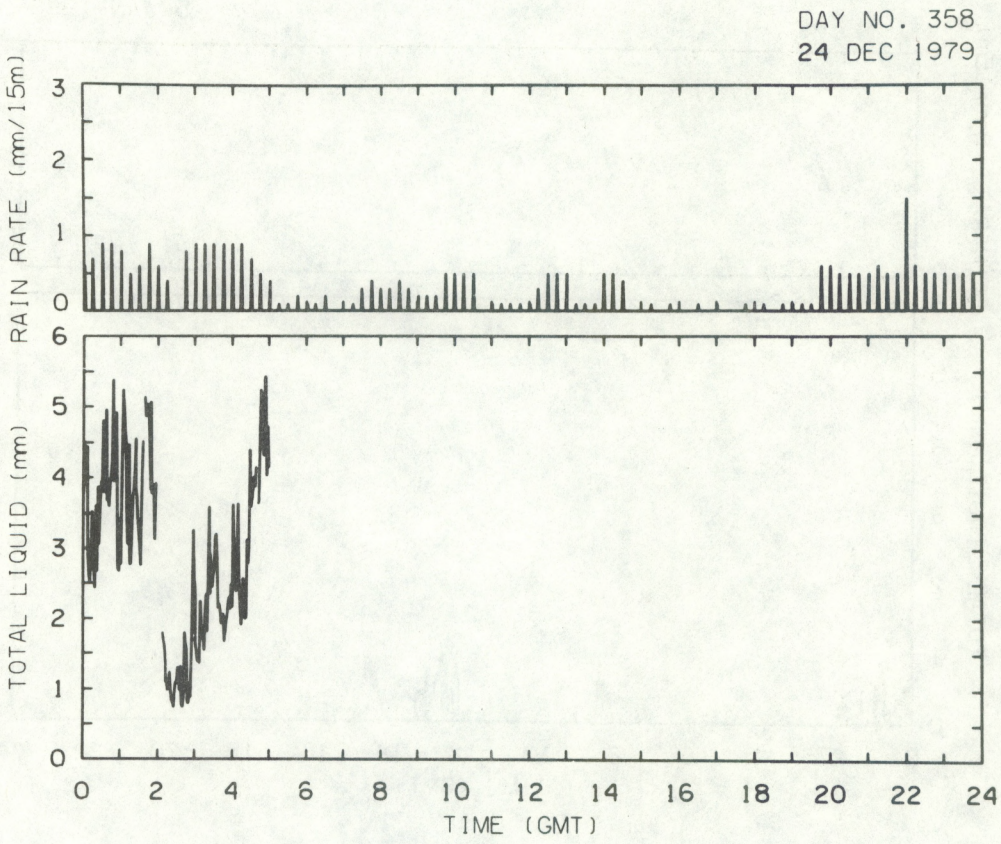
DAY NO. 358
24 DEC 1979
RAIN RATE (mm/15m)
TOTAL LIQUID (mm)
TIME (GMT)

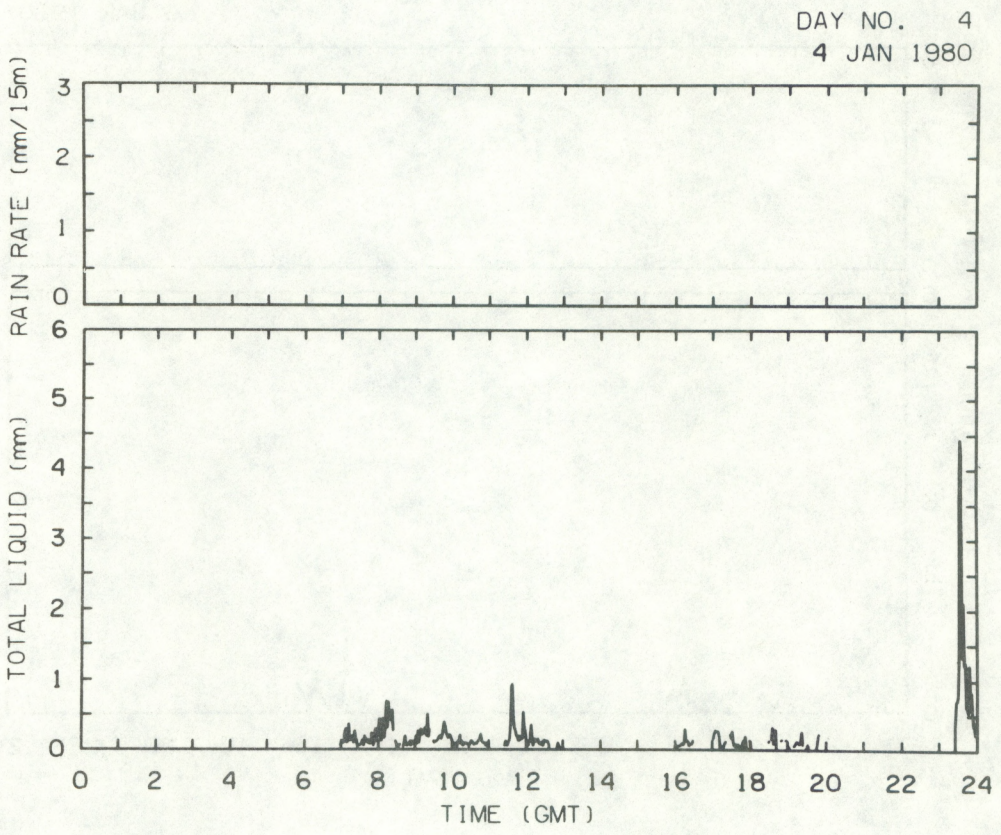
DAY NO. 4
4 JAN 1980
RAIN RATE (mm/15m)
TOTAL LIQUID (mm)
TIME (GMT)

Figure 7

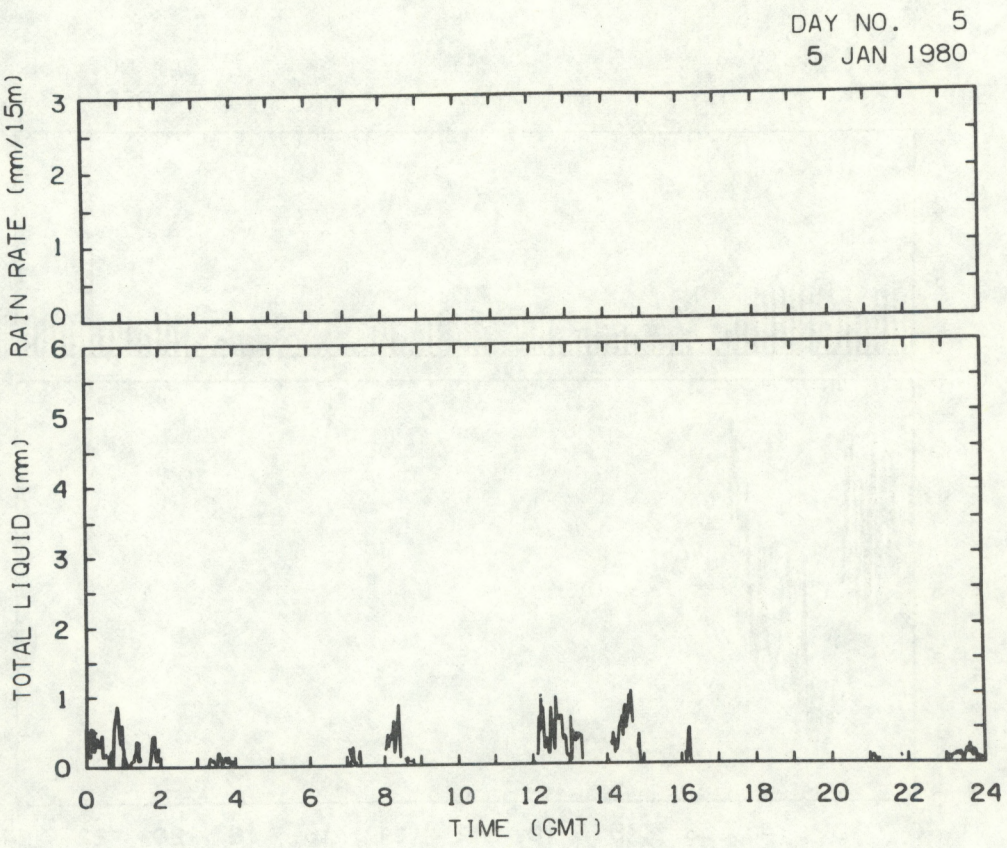
DAY NO. 5
5 JAN 1980
RAIN RATE (mm/15m)
TOTAL LIQUID (mm)
TIME (GMT)

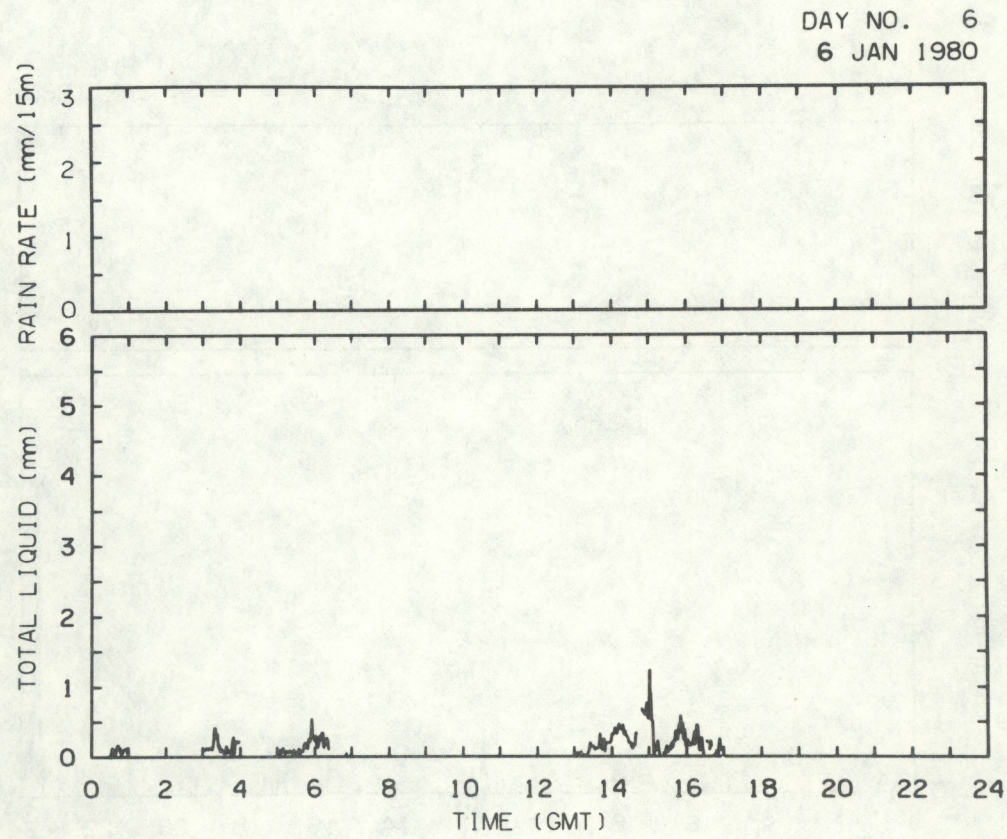
DAY NO. 6
6 JAN 1980
RAIN RATE (mm/15m)
TOTAL LIQUID (mm)
TIME (GMT)

Figure 8

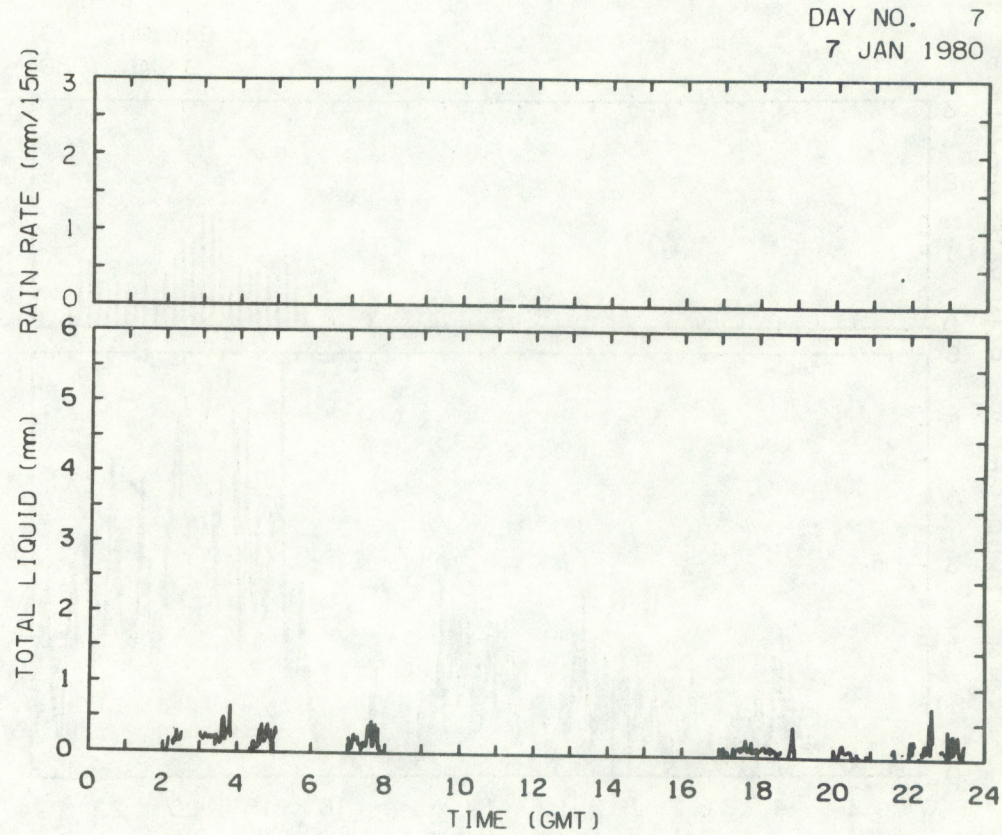
DAY NO. 7
7 JAN 1980
RAIN RATE (mm/15m)
TOTAL LIQUID (mm)
TIME (GMT)

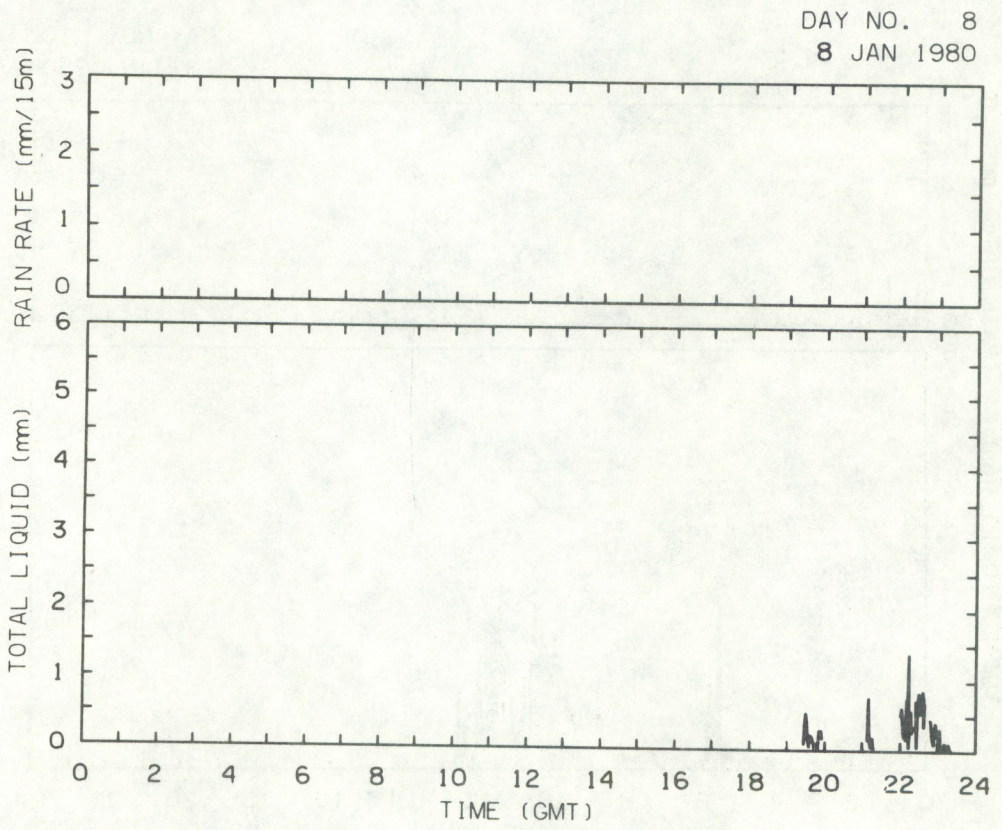
DAY NO. 8
8 JAN 1980
RAIN RATE (mm/15m)
TOTAL LIQUID (mm)
TIME (GMT)

Figure 9

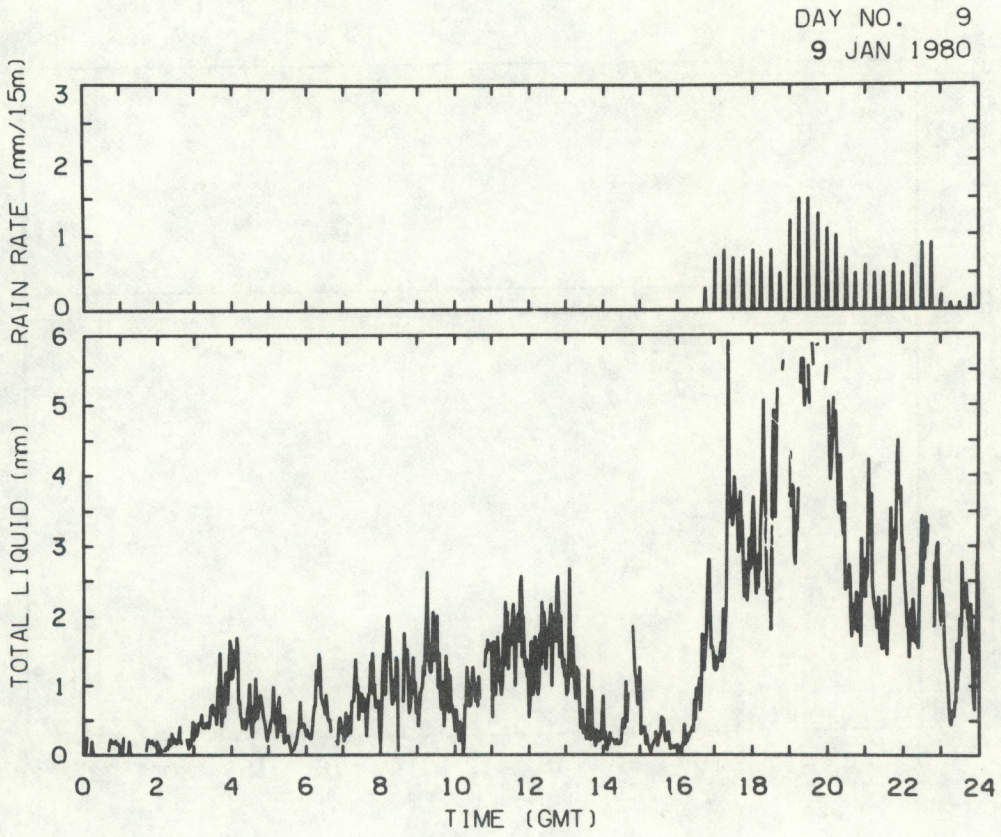
DAY NO. 9
9 JAN 1980
RAIN RATE (mm/15m)
TOTAL LIQUID (mm)
TIME (GMT)

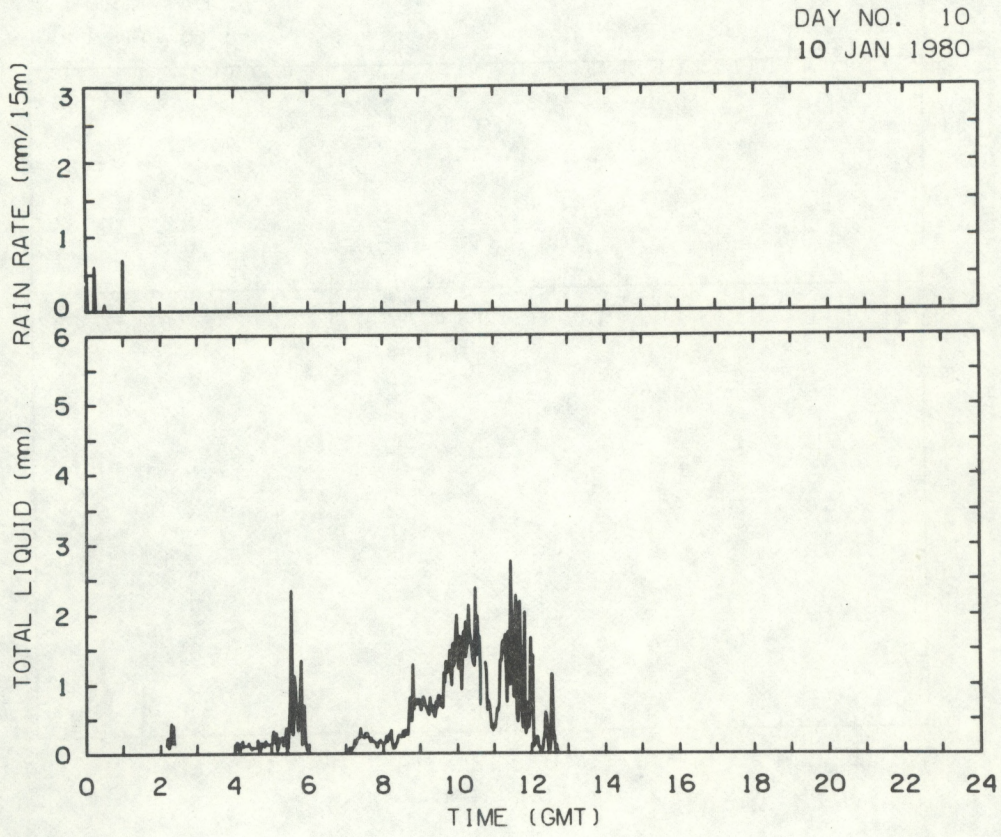
DAY NO. 10
10 JAN 1980
RAIN RATE (mm/15m)
TOTAL LIQUID (mm)
TIME (GMT)

Figure 10

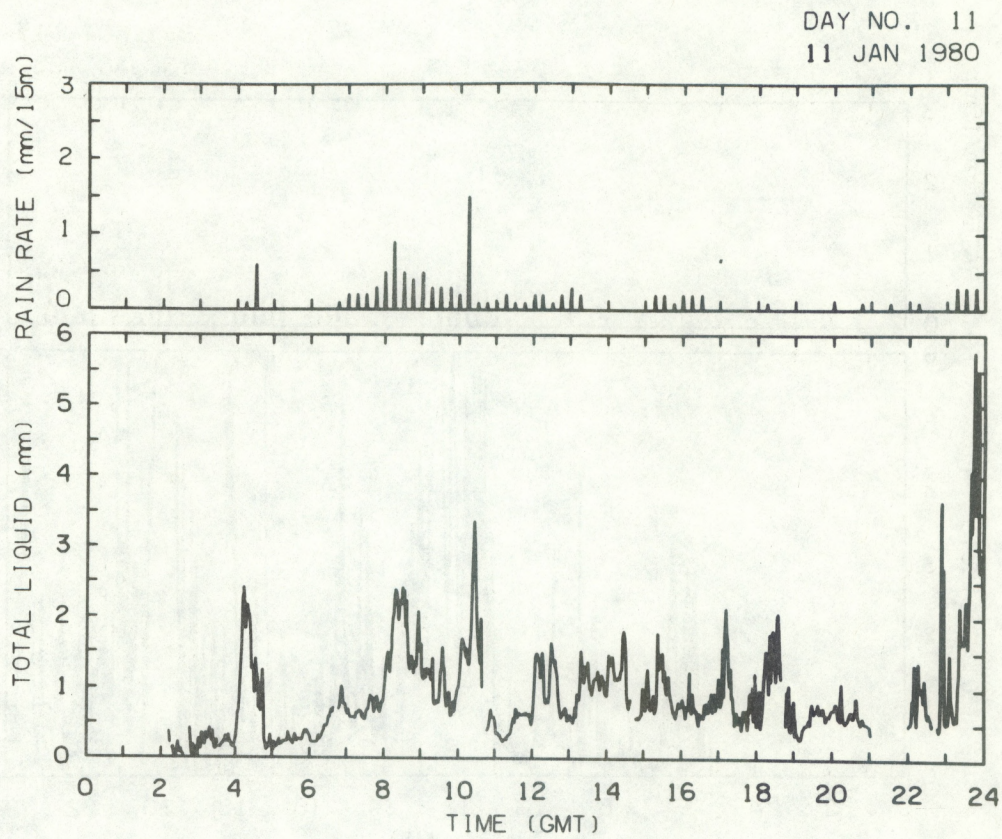
DAY NO. 11
11 JAN 1980
RAIN RATE (mm/15m)
TOTAL LIQUID (mm)
TIME (GMT)

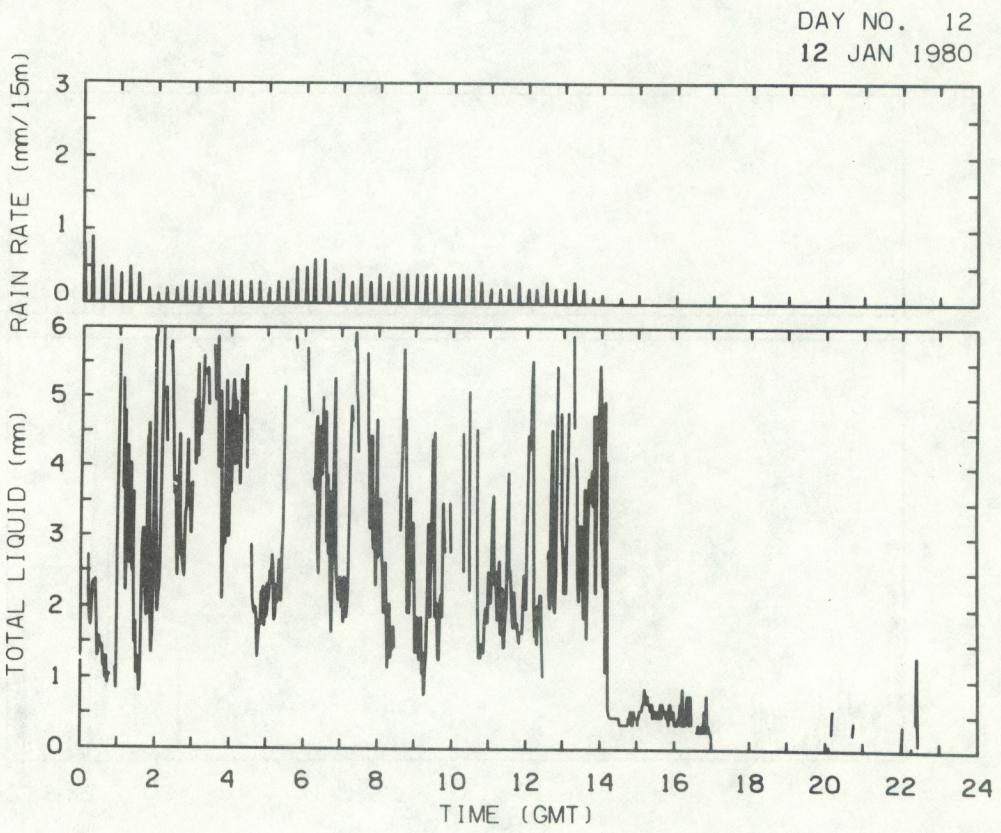
DAY NO. 12
12 JAN 1980
RAIN RATE (mm/15m)
TOTAL LIQUID (mm)
TIME (GMT)

Figure 11

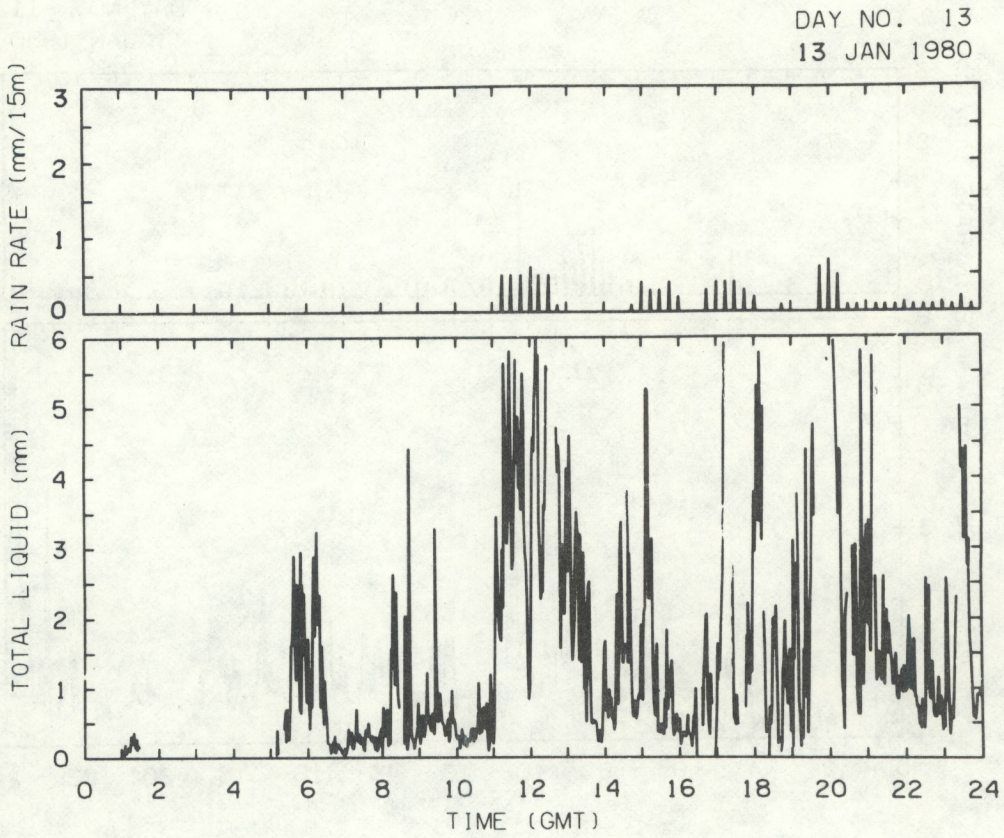
DAY NO. 13
13 JAN 1980
RAIN RATE (mm/15m)
TOTAL LIQUID (mm)
TIME (GMT)

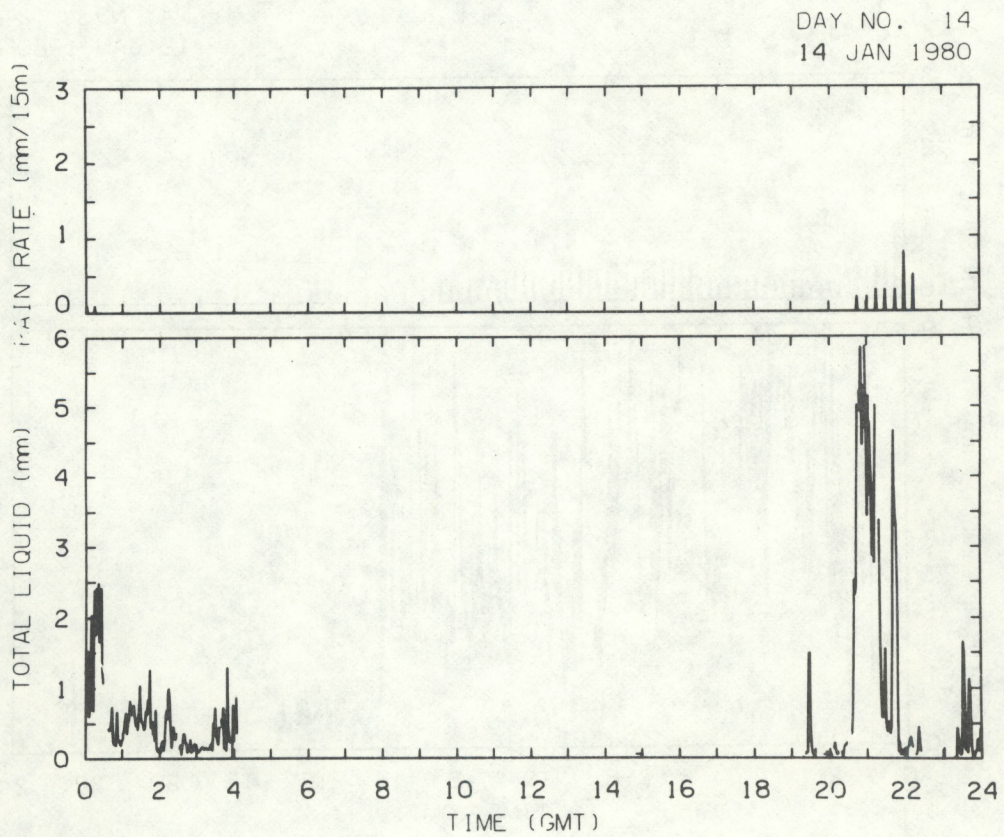
DAY NO. 14
14 JAN 1980
RAIN RATE (mm/15m)
TOTAL LIQUID (mm)
TIME (GMT)

Figure 12

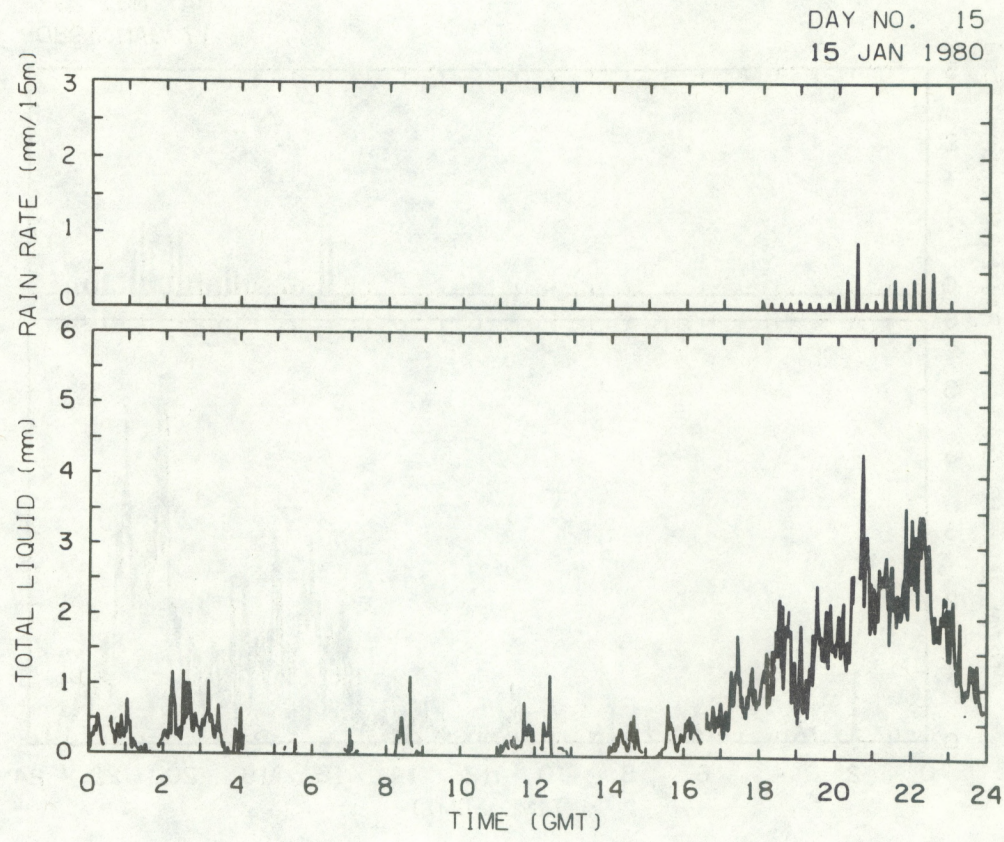
DAY NO. 15
15 JAN 1980
RAIN RATE (mm/15m)
TOTAL LIQUID (mm)
TIME (GMT)

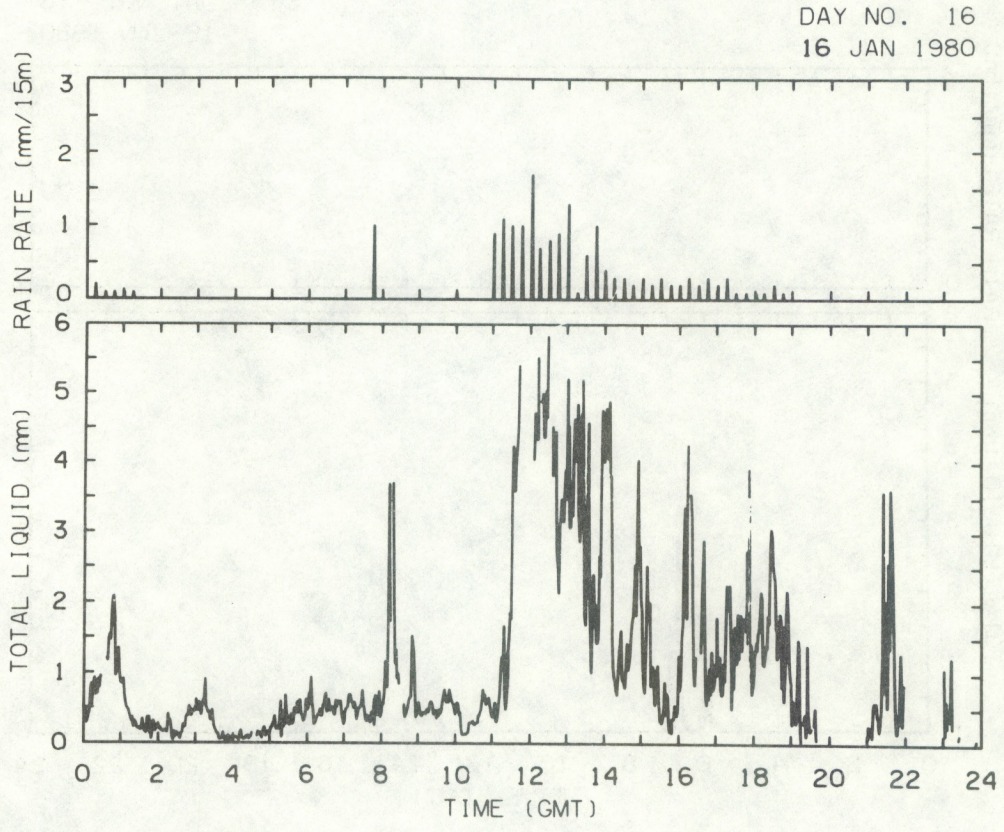
DAY NO. 16
16 JAN 1980
RAIN RATE (mm/15m)
TOTAL LIQUID (mm)
TIME (GMT)

Figure 13

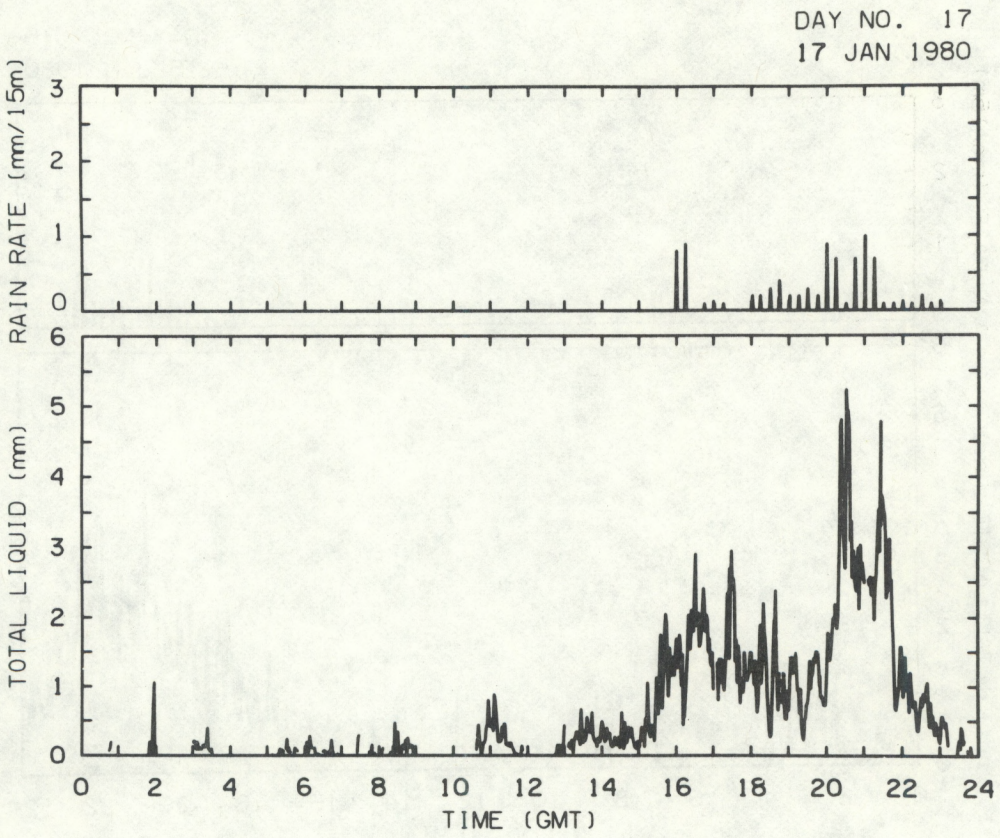
DAY NO. 17
17 JAN 1980
RAIN RATE (mm/15m)
TOTAL LIQUID (mm)
TIME (GMT)

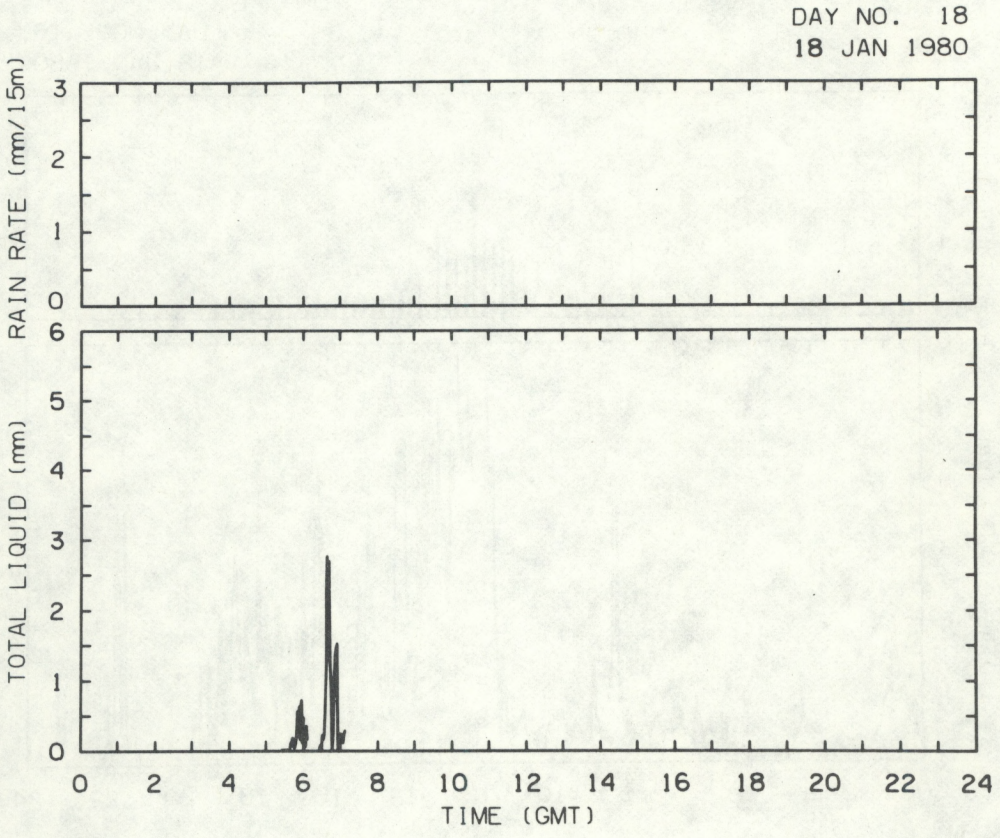
DAY NO. 18
18 JAN 1980
RAIN RATE (mm/15m)
TOTAL LIQUID (mm)
TIME (GMT)

Figure 14

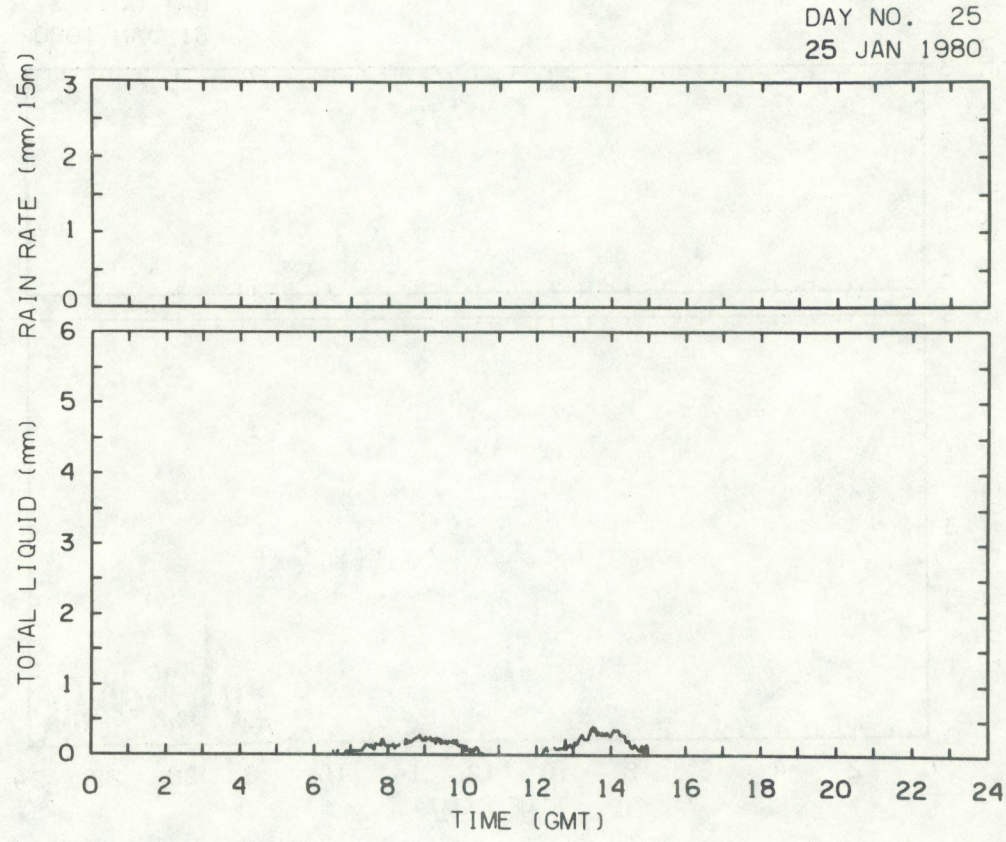
DAY NO. 25
25 JAN 1980
RAIN RATE (mm/15m)
TOTAL LIQUID (mm)
TIME (GMT)

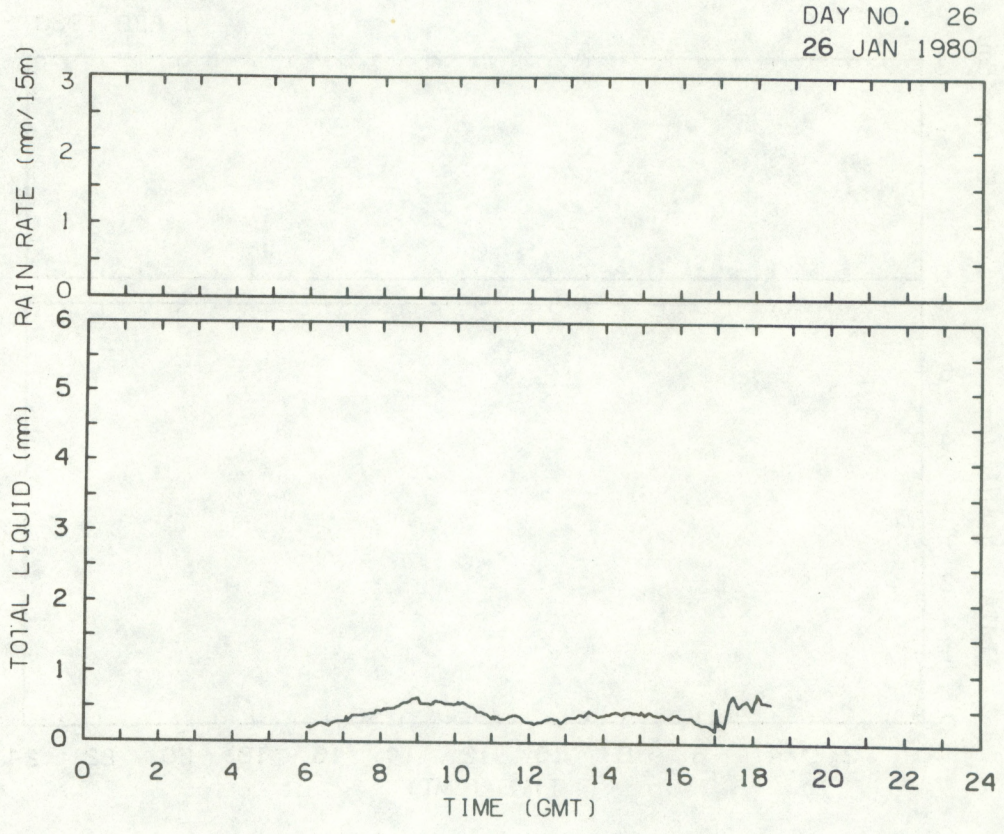
DAY NO. 26
26 JAN 1980
RAIN RATE (mm/15m)
TOTAL LIQUID (mm)
TIME (GMT)

Figure 15

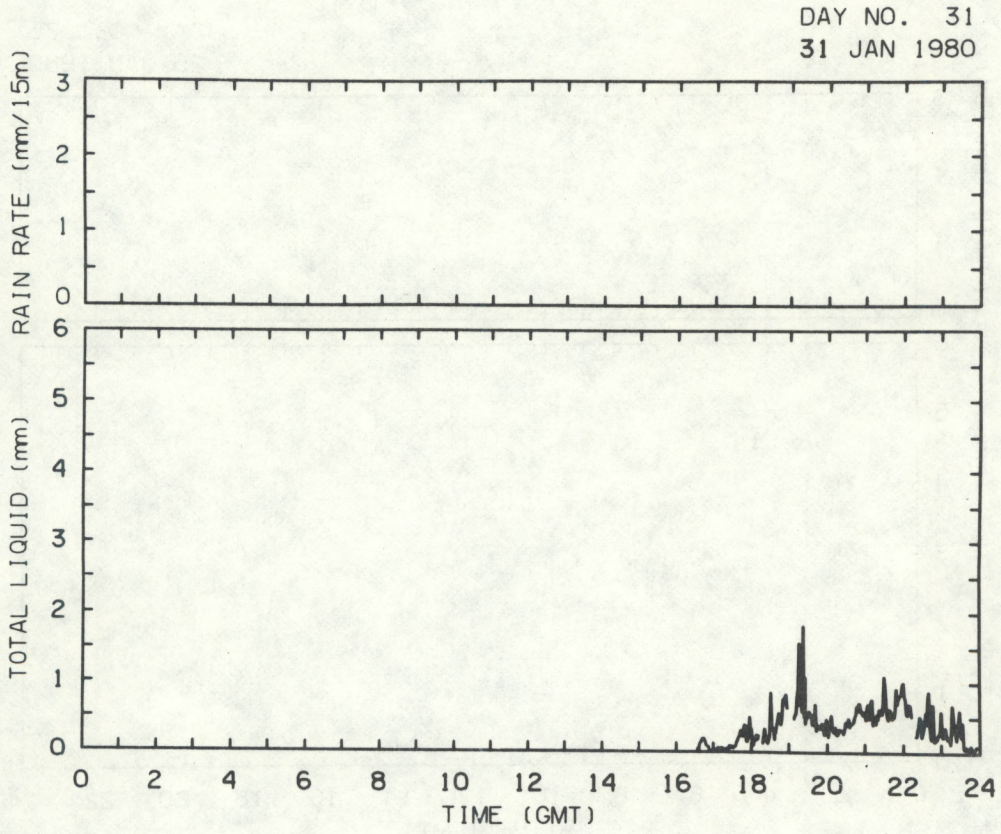
DAY NO. 31
31 JAN 1980
RAIN RATE (mm/15m)
TOTAL LIQUID (mm)
TIME (GMT)

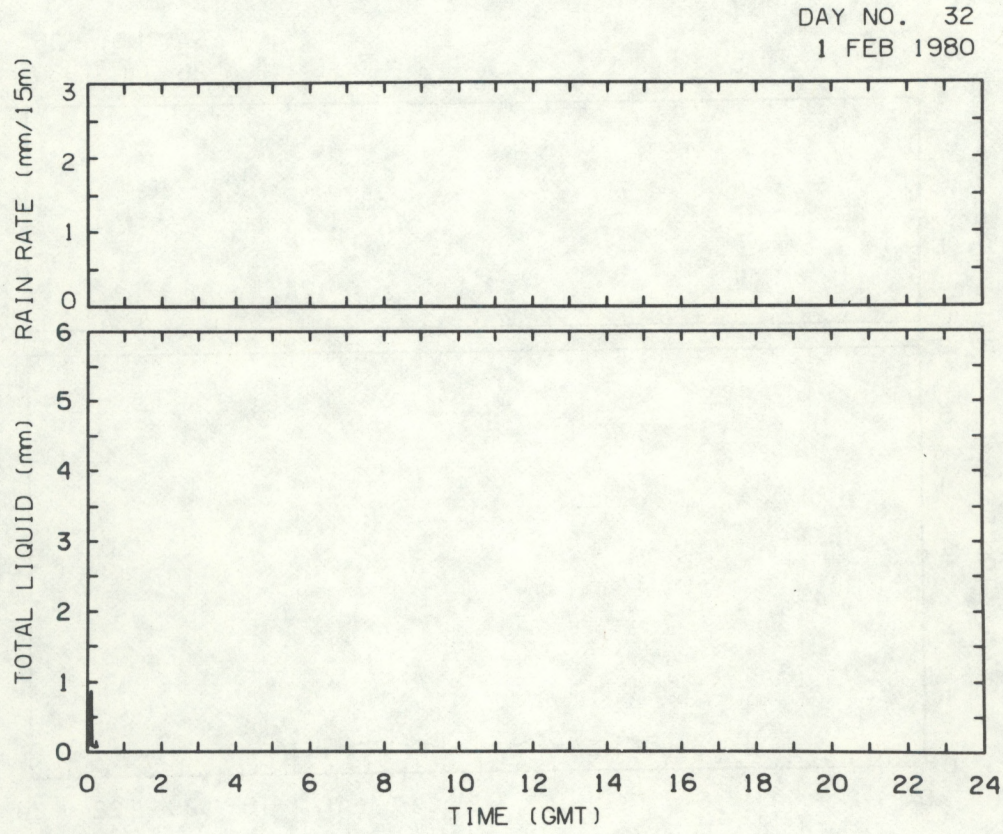
DAY NO. 32
1 FEB 1980
RAIN RATE (mm/15m)
TOTAL LIQUID (mm)
TIME (GMT)

Figure 16

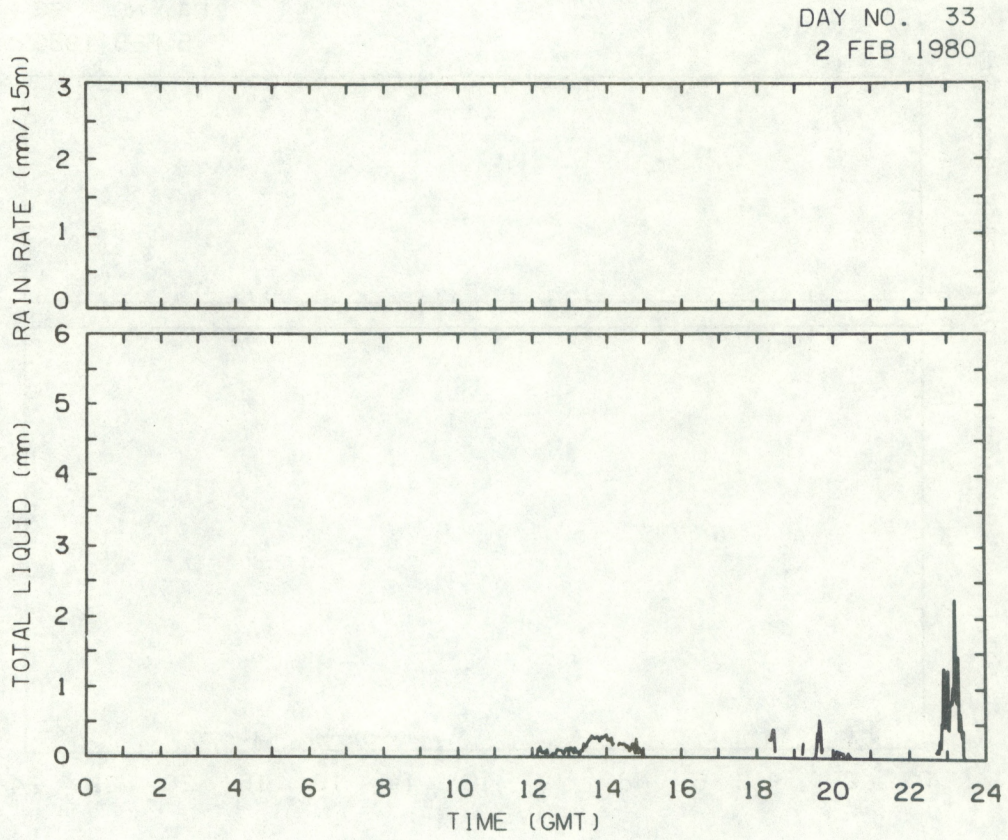
DAY NO. 33
2 FEB 1980
RAIN RATE (mm/15m)
TOTAL LIQUID (mm)
TIME (GMT)

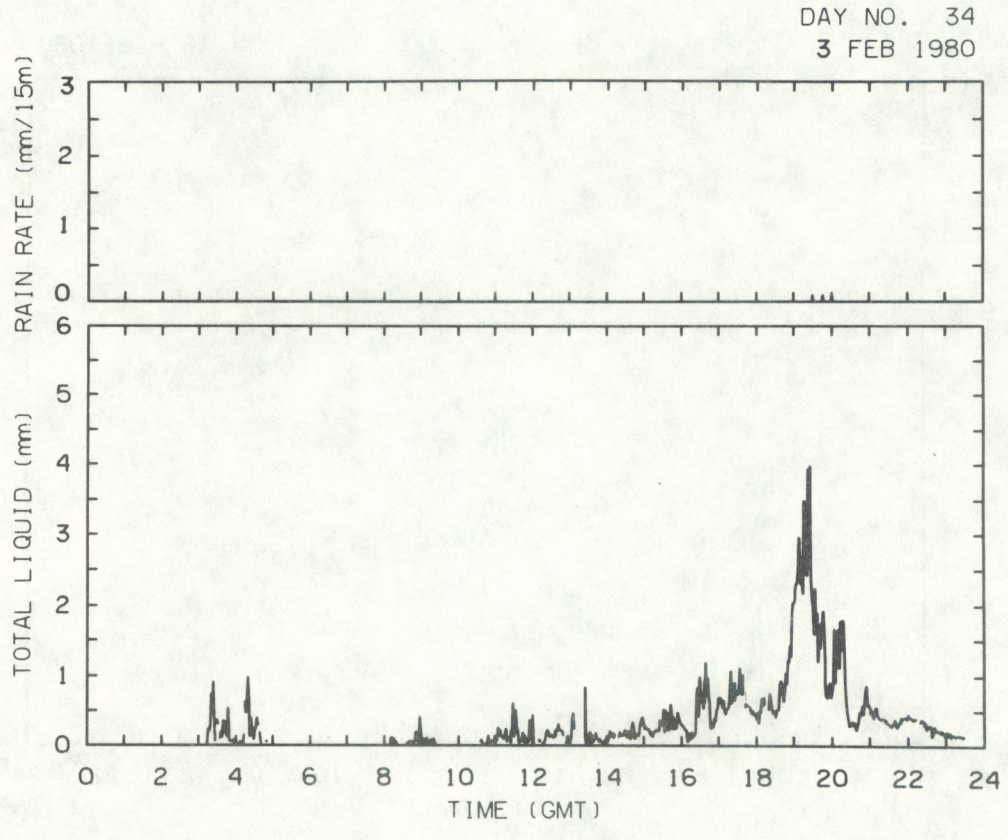
DAY NO. 34
3 FEB 1980
RAIN RATE (mm/15m)
TOTAL LIQUID (mm)
TIME (GMT)

Figure 17

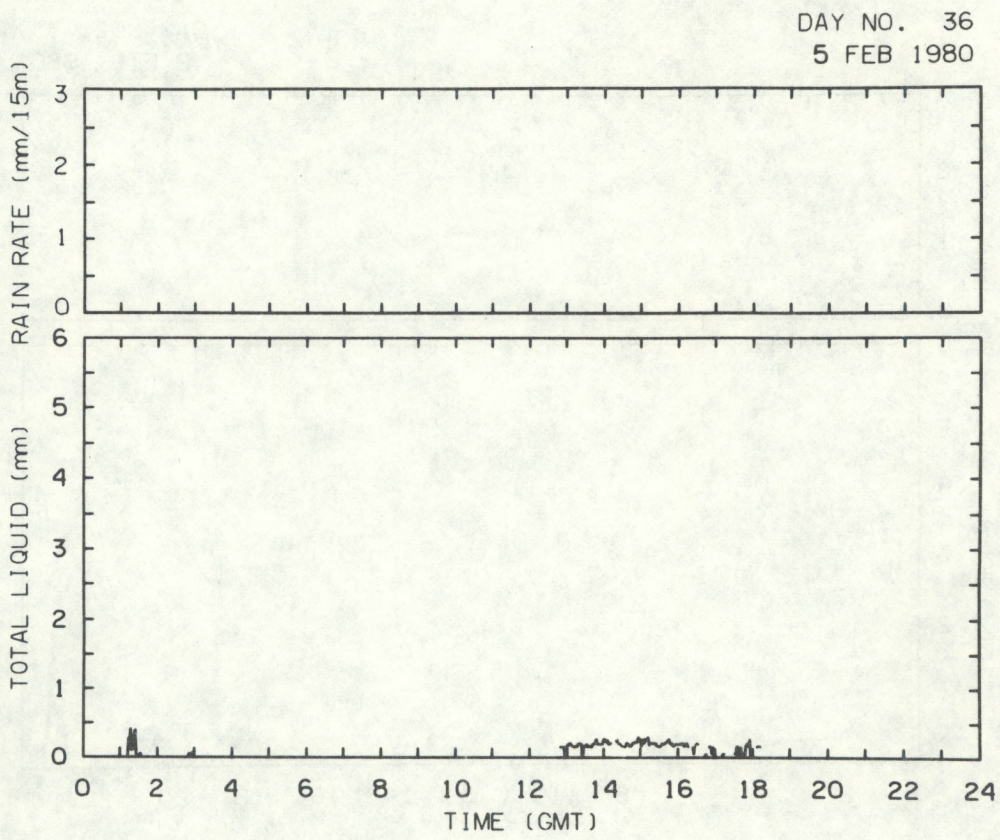
DAY NO. 36
5 FEB 1980
RAIN RATE (mm/15m)
TOTAL LIQUID (mm)
TIME (GMT)

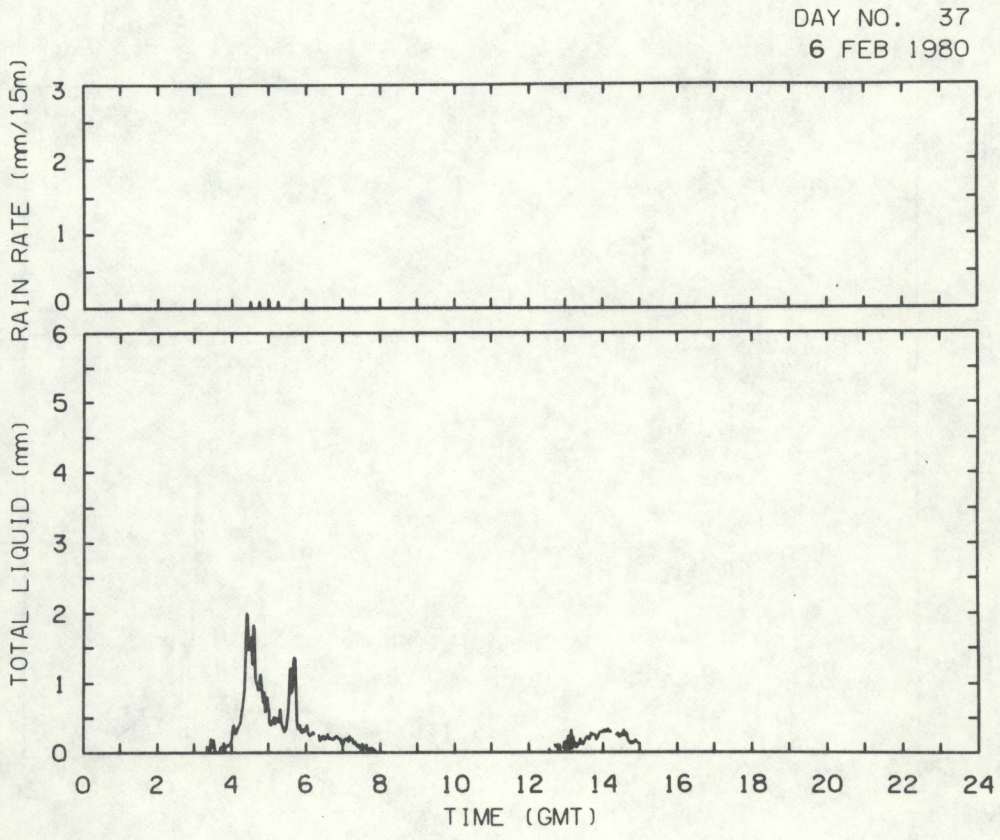
DAY NO. 37
6 FEB 1980
RAIN RATE (mm/15m)
TOTAL LIQUID (mm)
TIME (GMT)

Figure 18

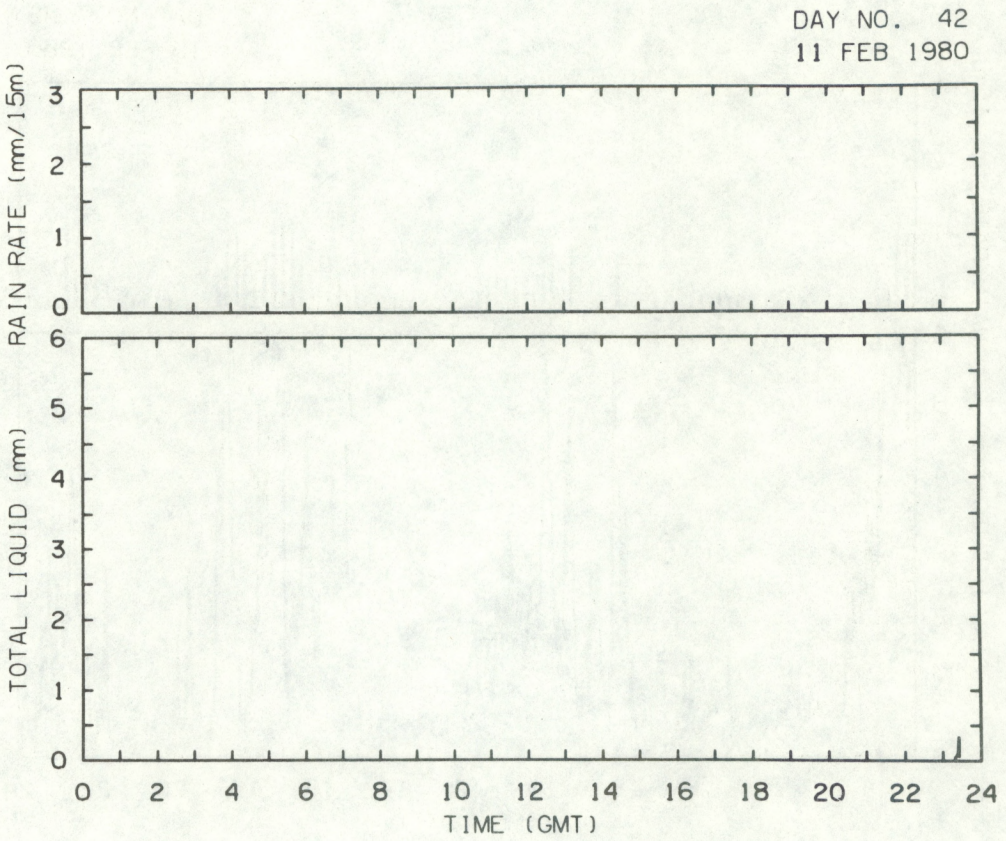
DAY NO. 42
11 FEB 1980
RAIN RATE (mm/15m)
TOTAL LIQUID (mm)
TIME (GMT)

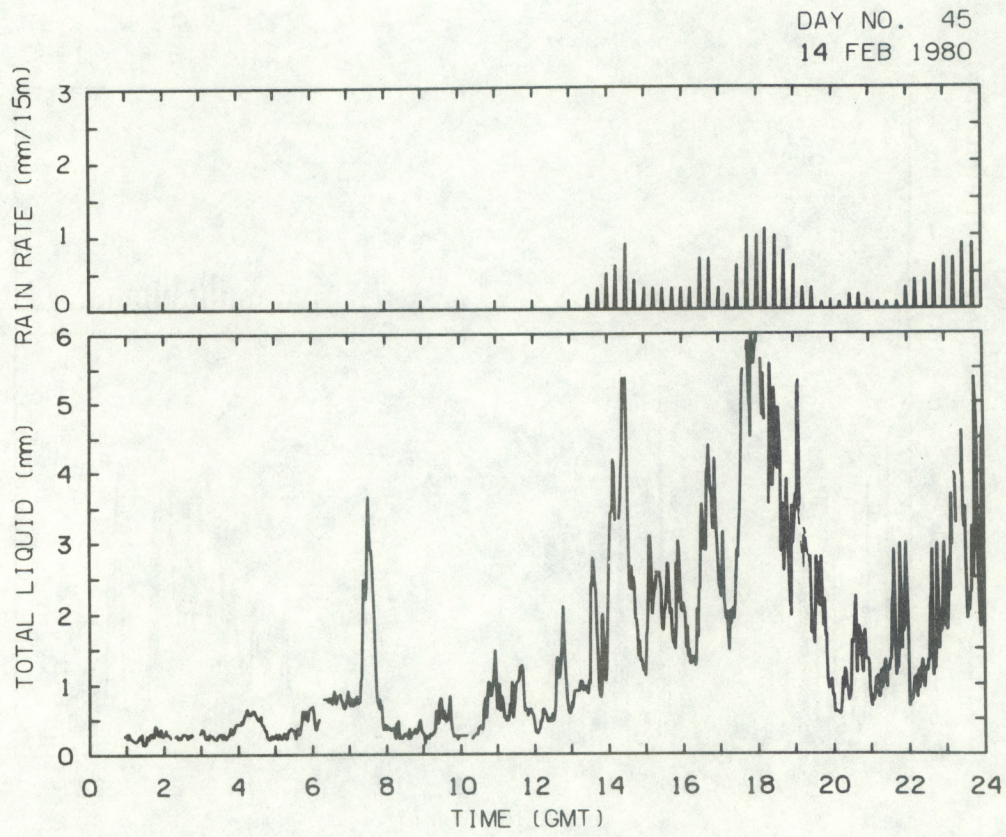
DAY NO. 45
14 FEB 1980
RAIN RATE (mm/15m)
TOTAL LIQUID (mm)
TIME (GMT)

Figure 19

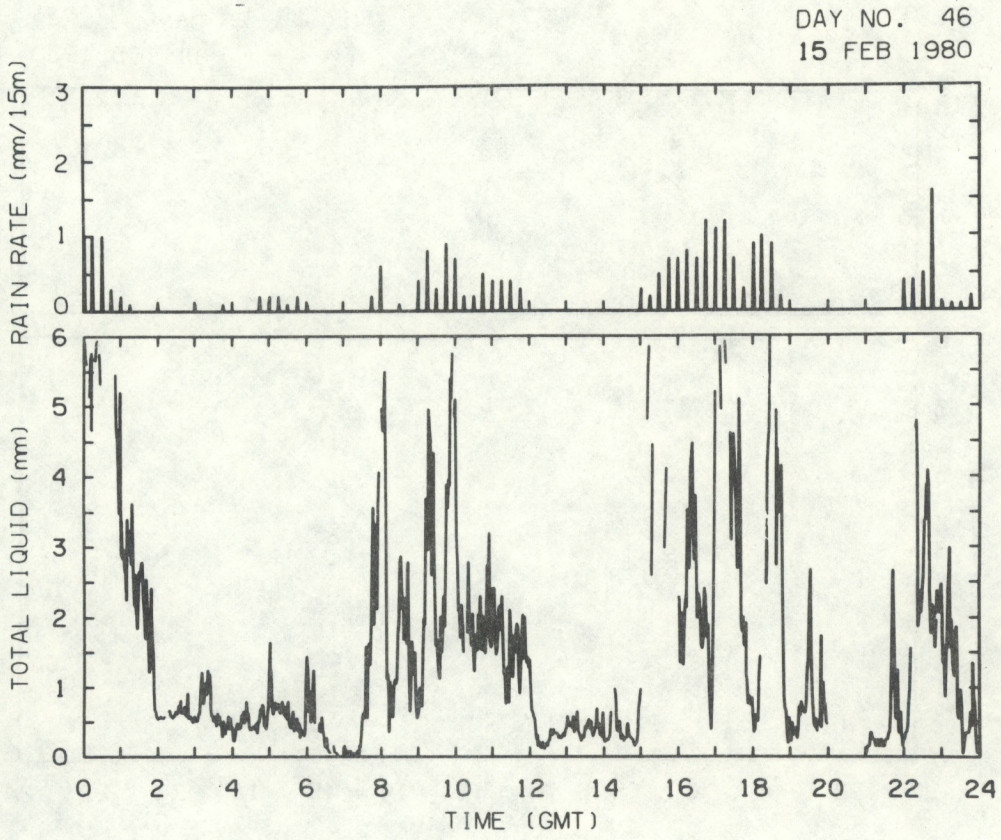
DAY NO. 46
15 FEB 1980
RAIN RATE (mm/15m)
TOTAL LIQUID (mm)
TIME (GMT)

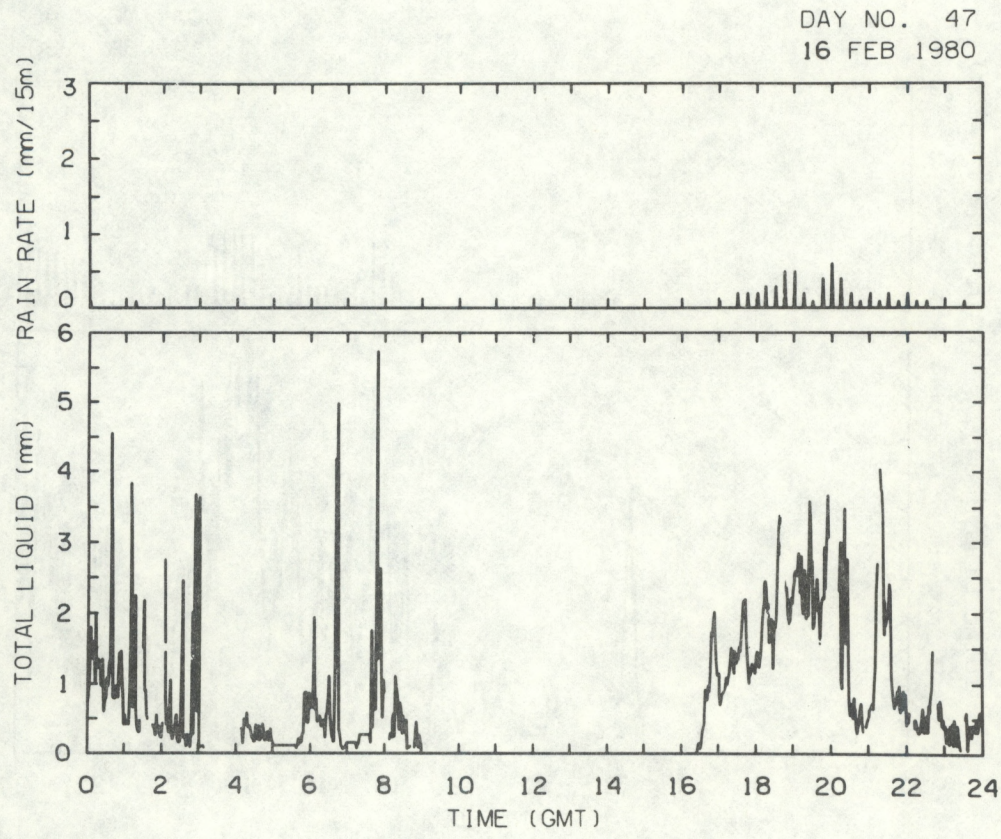
DAY NO. 47
16 FEB 1980
RAIN RATE (mm/15m)
TOTAL LIQUID (mm)
TIME (GMT)

Figure 20

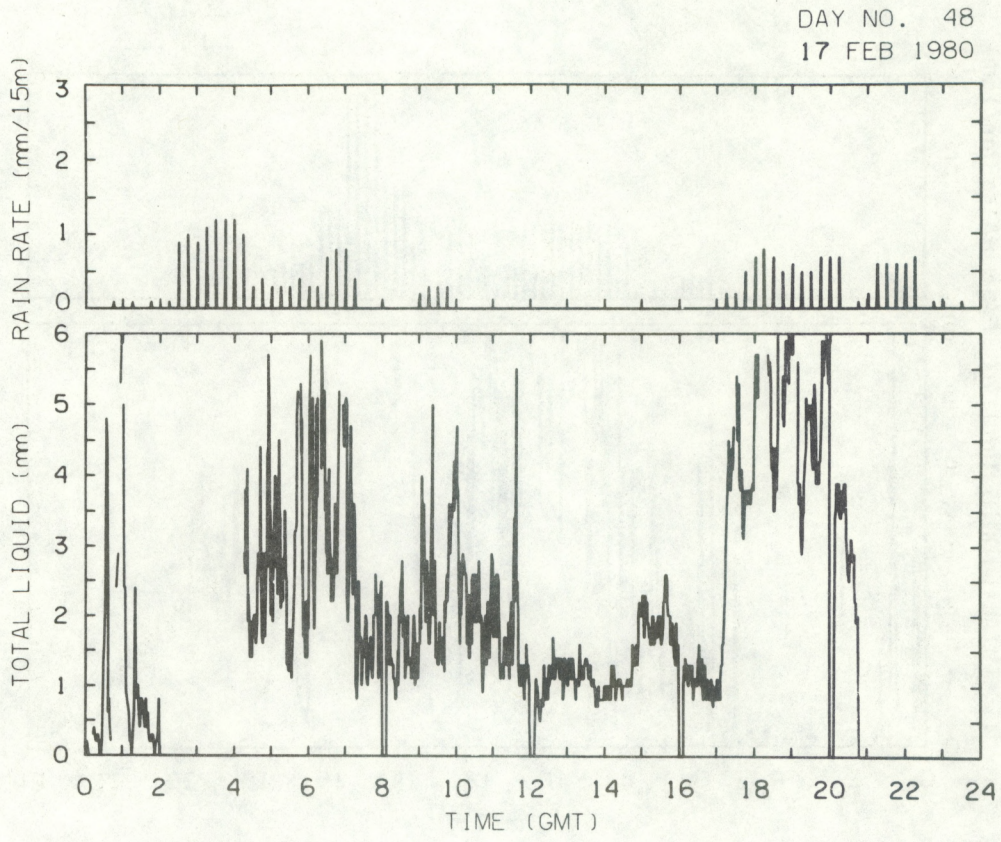
DAY NO. 48
17 FEB 1980
RAIN RATE (mm/15m)
TOTAL LIQUID (mm)
TIME (GMT)

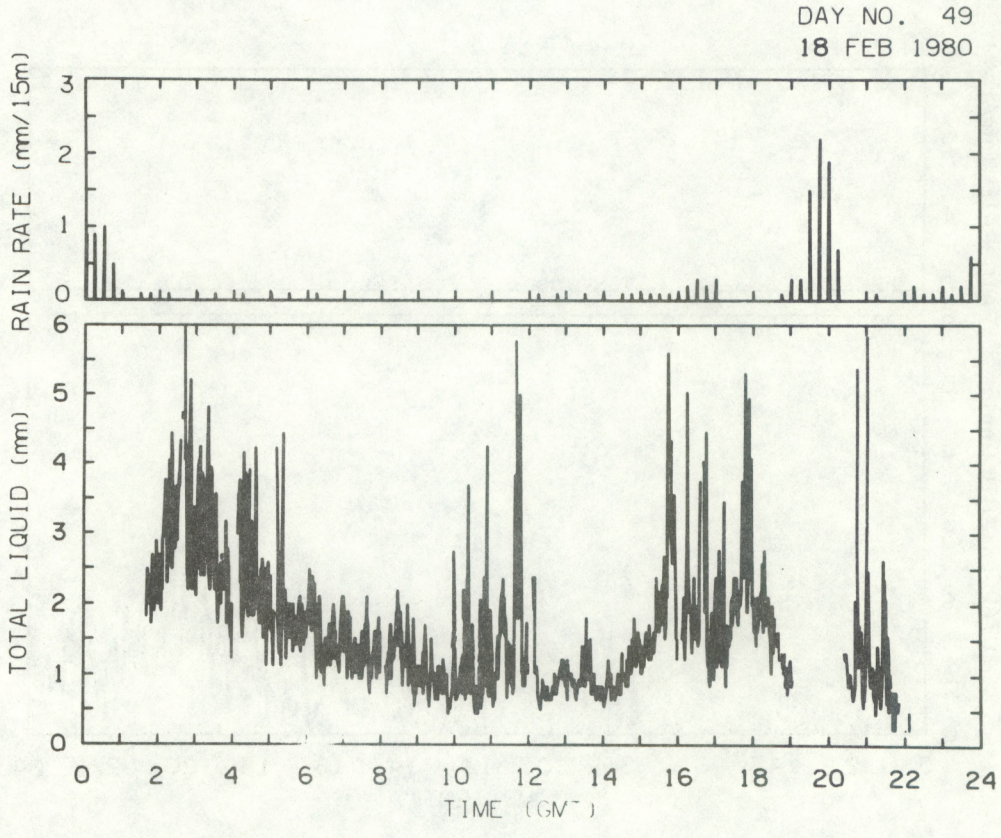
DAY NO. 49
18 FEB 1980
RAIN RATE (mm/15m)
TOTAL LIQUID (mm)
TIME (GMT)

Figure 21

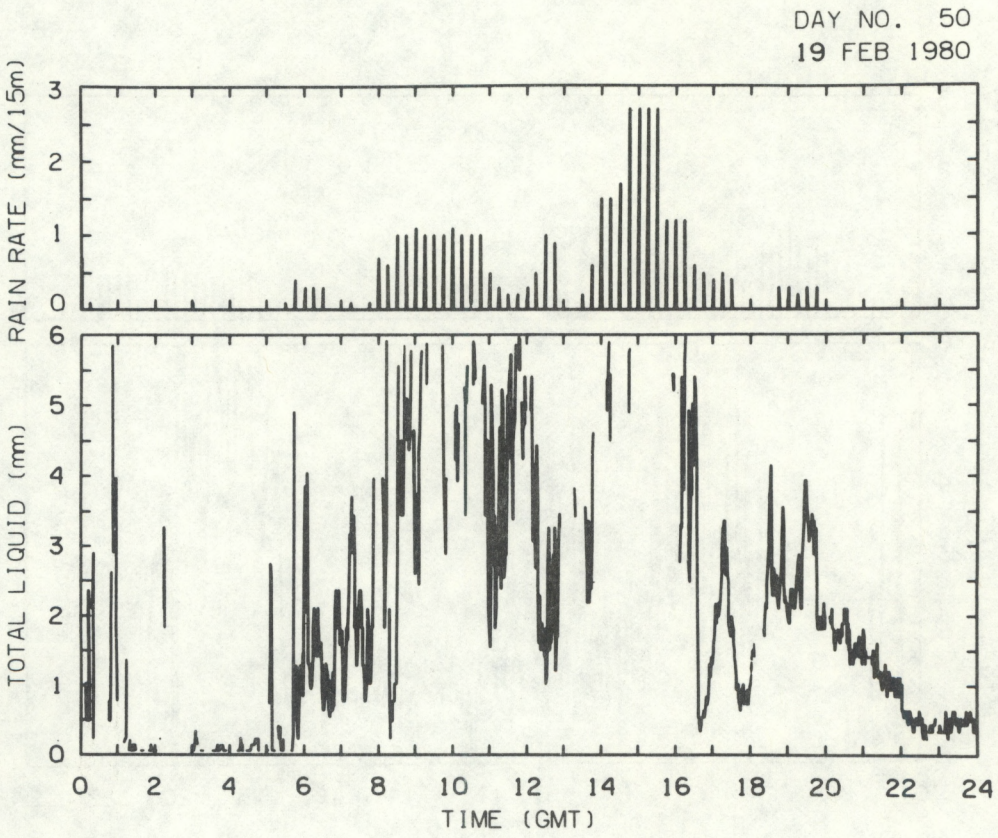
DAY NO. 50
19 FEB 1980
RAIN RATE (mm/15m)
TOTAL LIQUID (mm)
TIME (GMT)

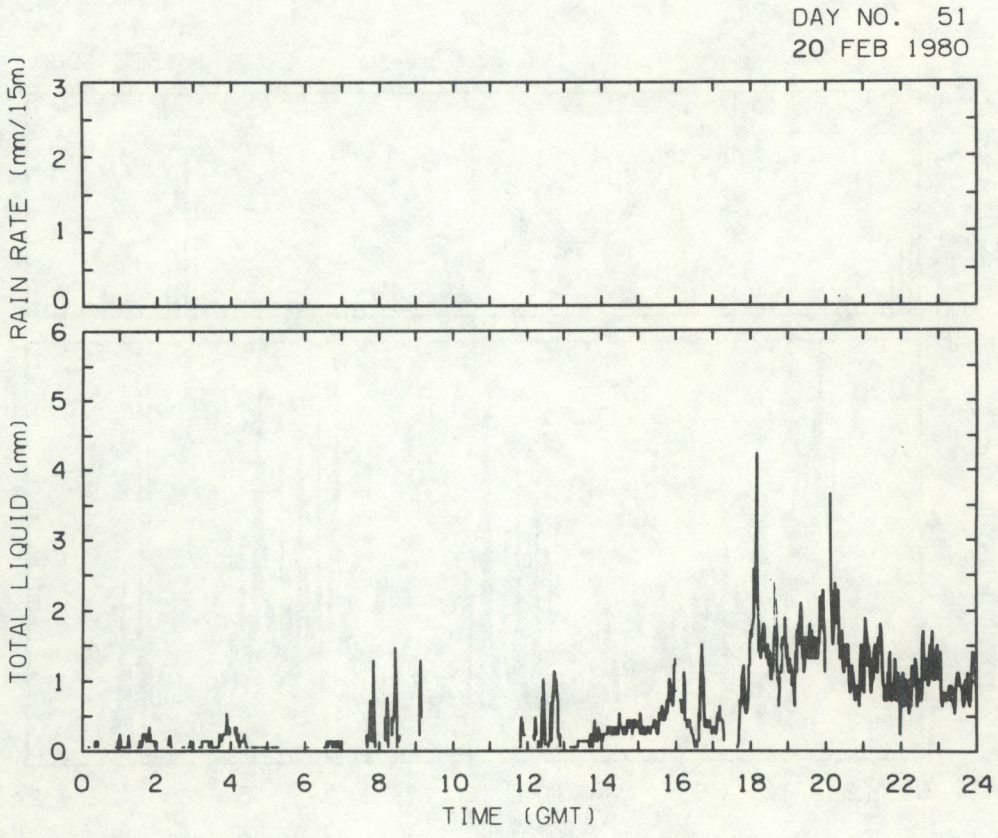
DAY NO. 51
20 FEB 1980
RAIN RATE (mm/15m)
TOTAL LIQUID (mm)
TIME (GMT)

Figure 22

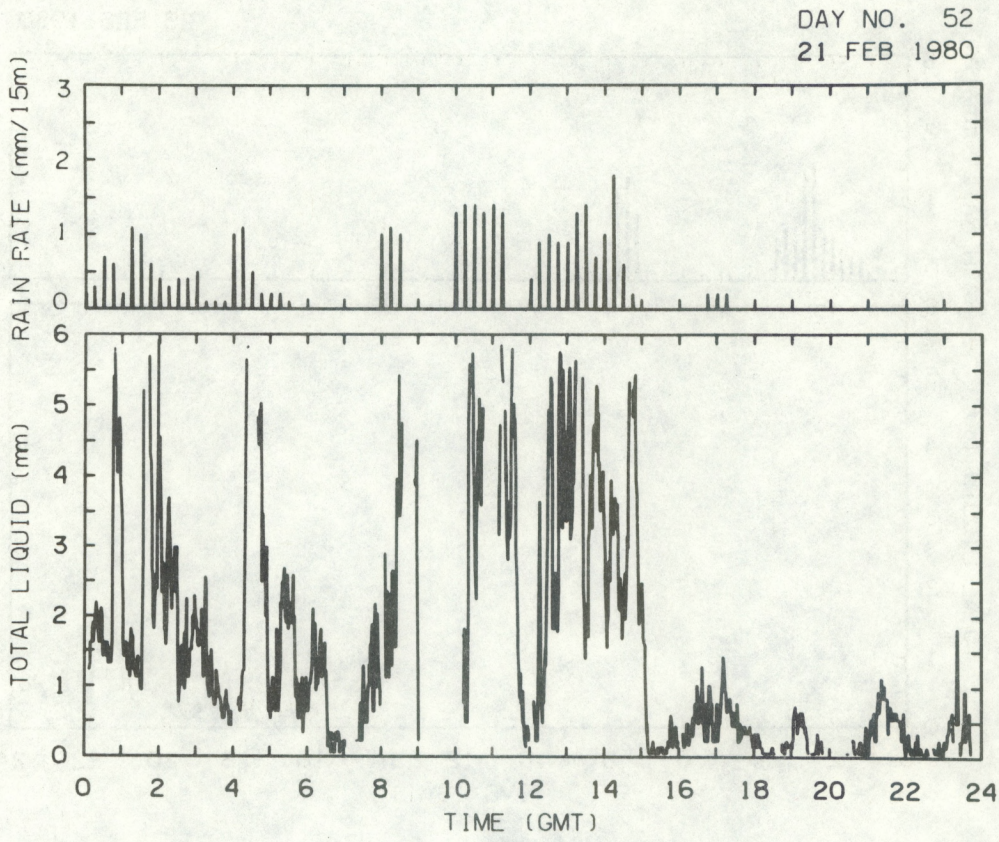
DAY NO. 52
21 FEB 1980
RAIN RATE (mm/15m)
TOTAL LIQUID (mm)
TIME (GMT)

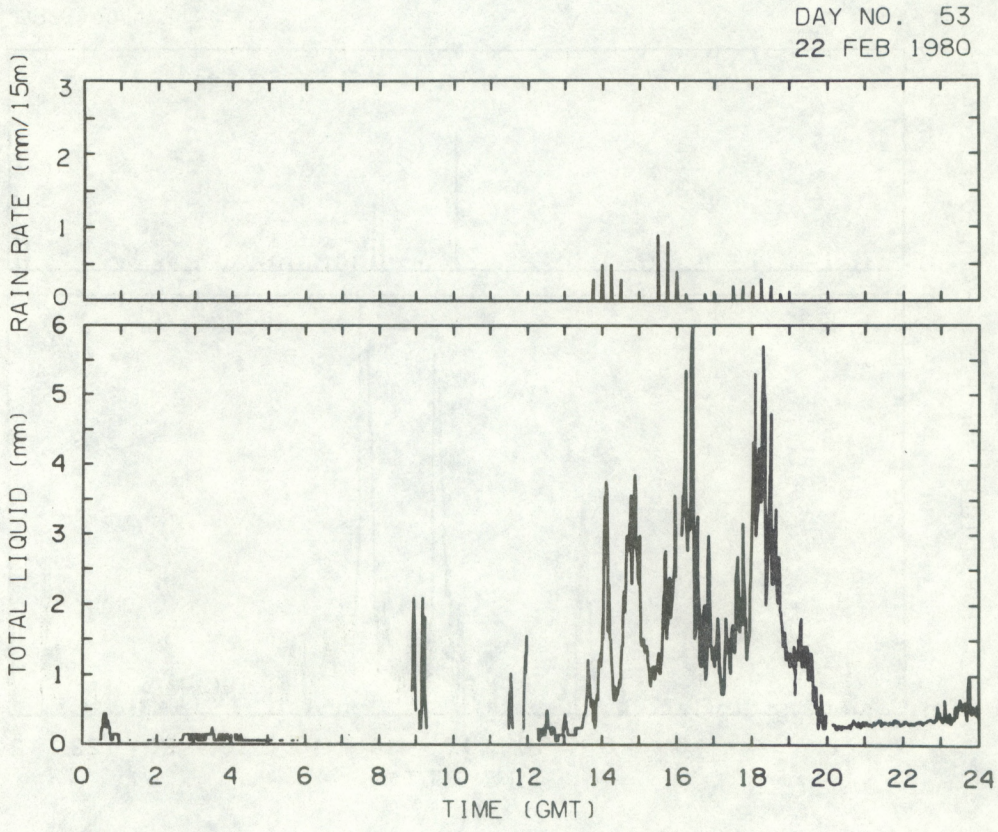
DAY NO. 53
22 FEB 1980
RAIN RATE (mm/15m)
TOTAL LIQUID (mm)
TIME (GMT)

Figure 23

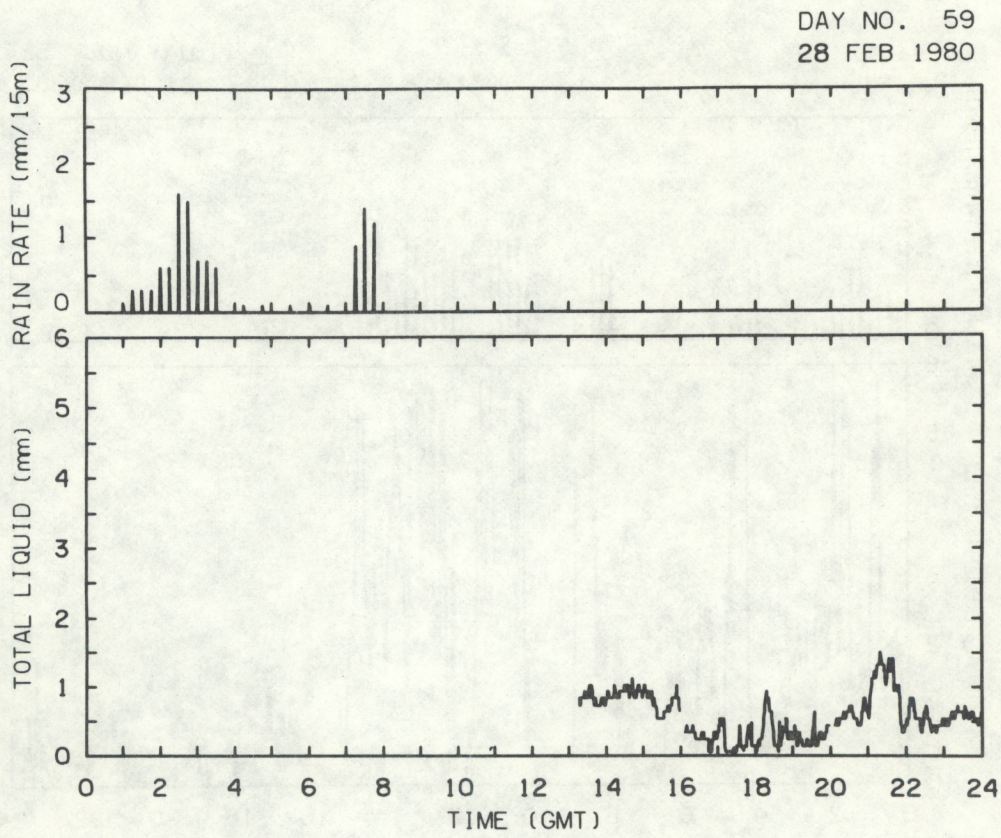
DAY NO. 59
28 FEB 1980
RAIN RATE (mm/15m)
TOTAL LIQUID (mm)
TIME (GMT)

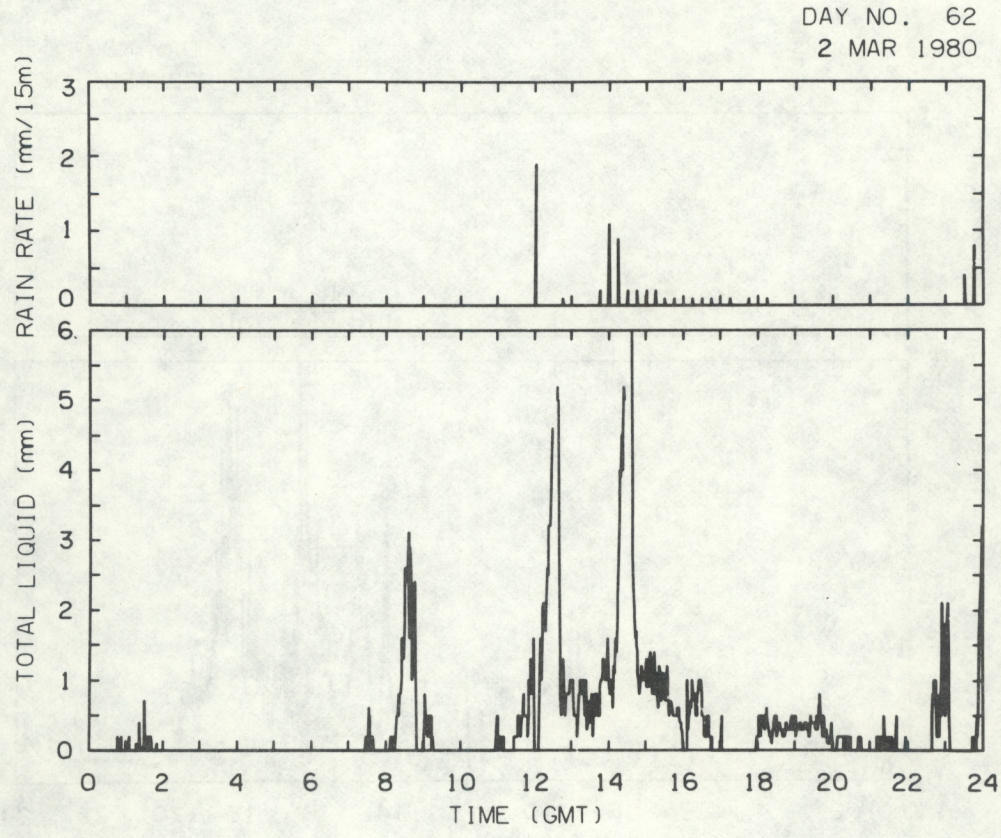
DAY NO. 62
2 MAR 1980
RAIN RATE (mm/15m)
TOTAL LIQUID (mm)
TIME (GMT)

Figure 24

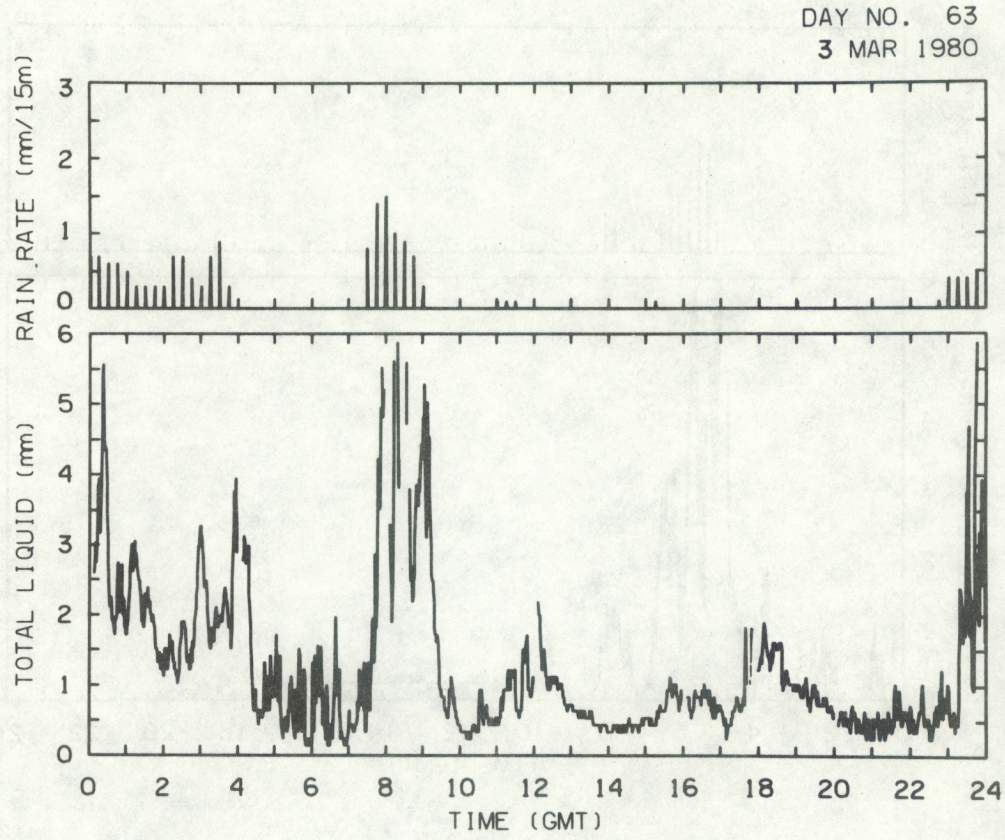
DAY NO. 63
3 MAR 1980
RAIN RATE (mm/15m)
TOTAL LIQUID (mm)
TIME (GMT)

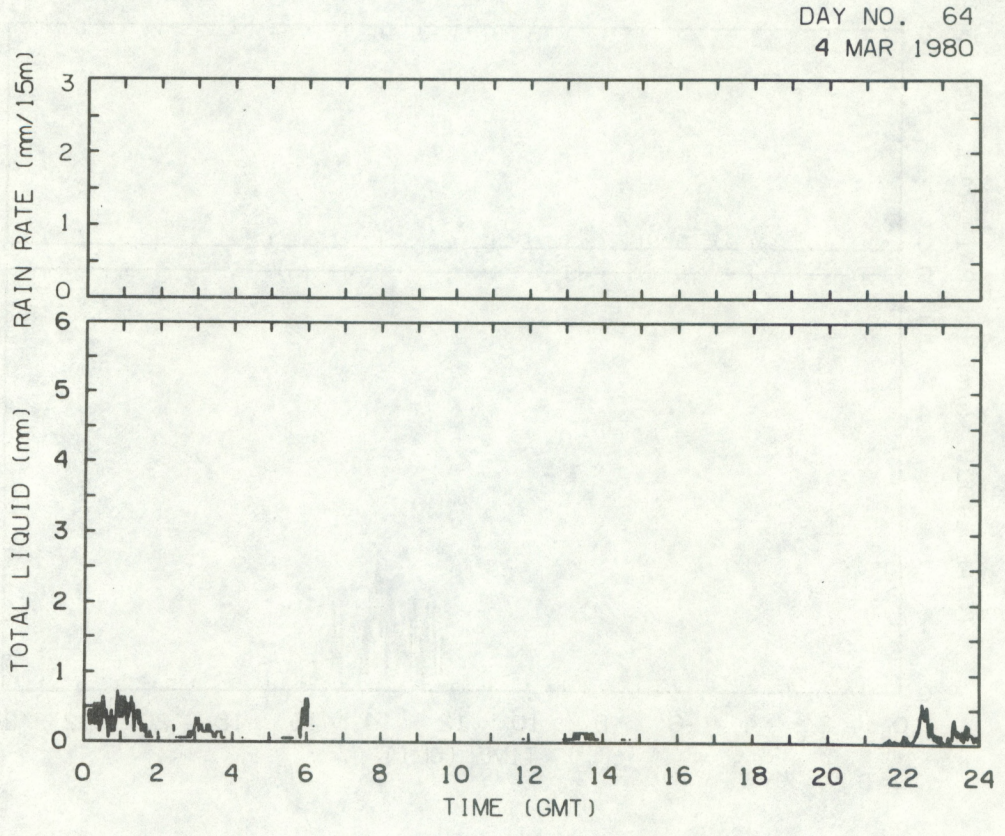
DAY NO. 64
4 MAR 1980
RAIN RATE (mm/15m)
TOTAL LIQUID (mm)
TIME (GMT)

Figure 25

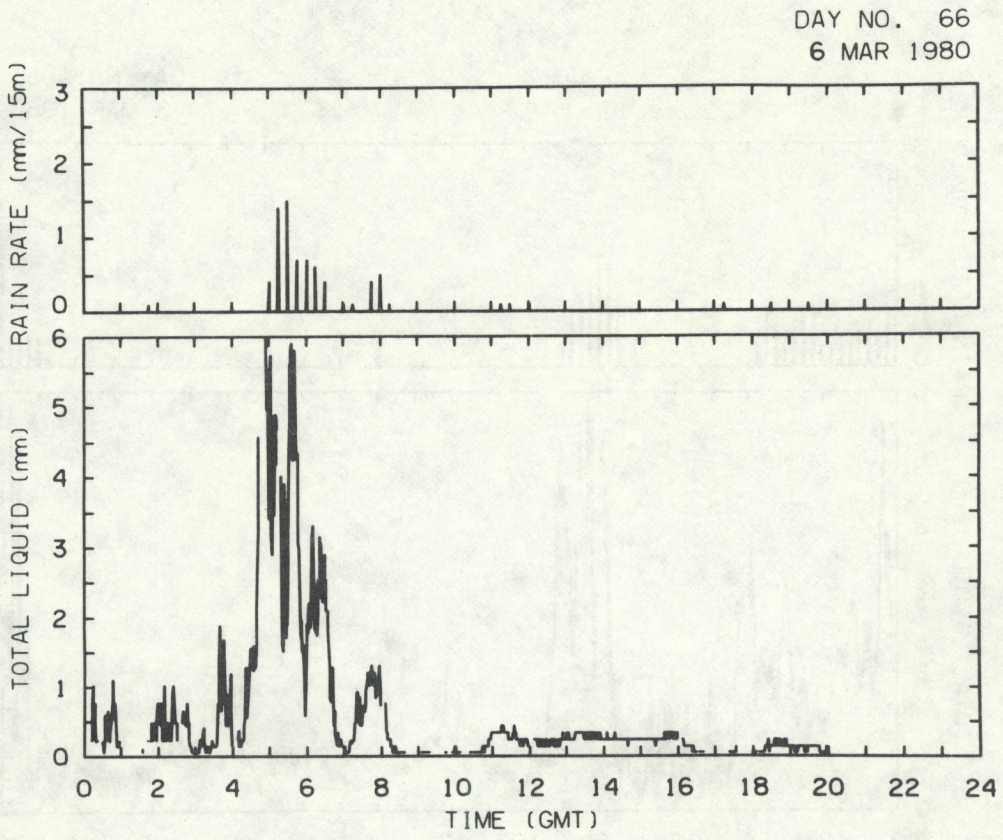
DAY NO. 66
6 MAR 1980
RAIN RATE (mm/15m)
TOTAL LIQUID (mm)
TIME (GMT)

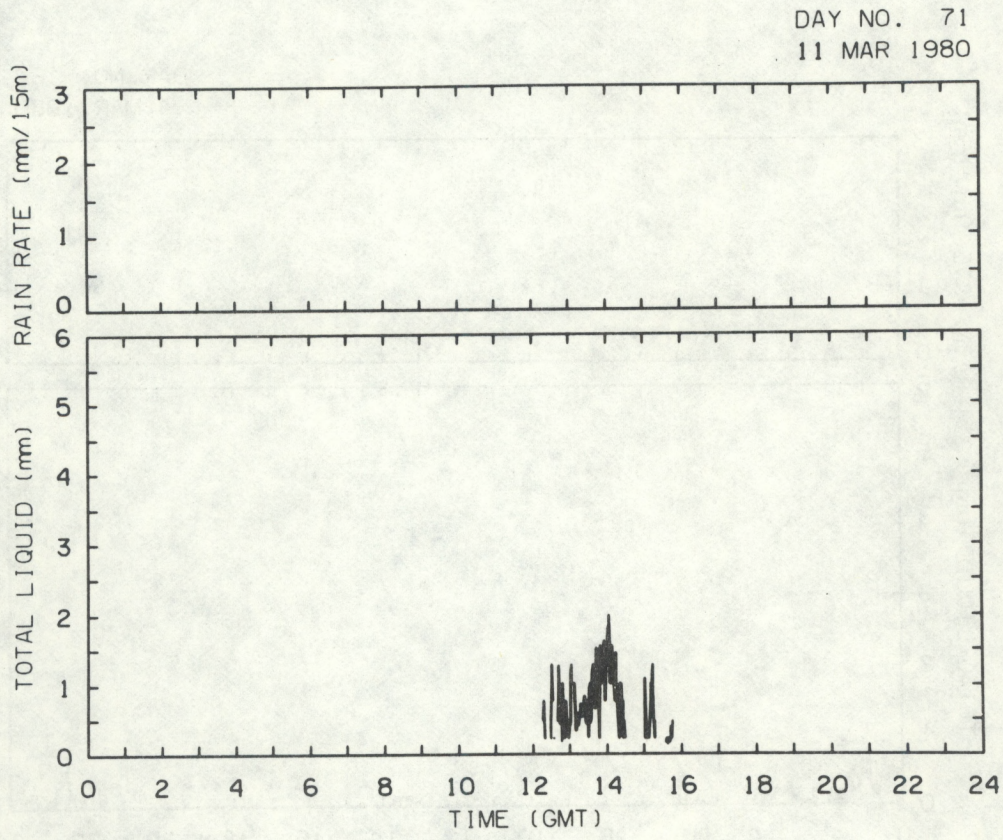
DAY NO. 71
11 MAR 1980
RAIN RATE (mm/15m)
TOTAL LIQUID (mm)
TIME (GMT)

Figure 26

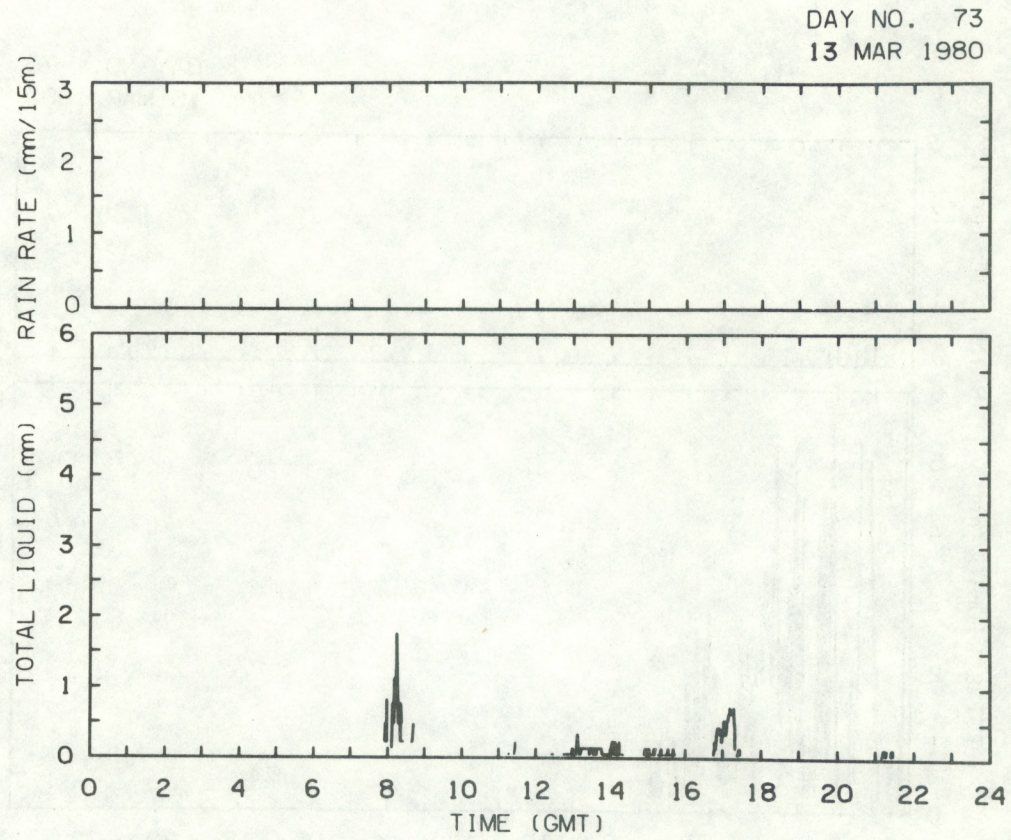
DAY NO. 73
13 MAR 1980
RAIN RATE (mm/15m)
TOTAL LIQUID (mm)
TIME (GMT)

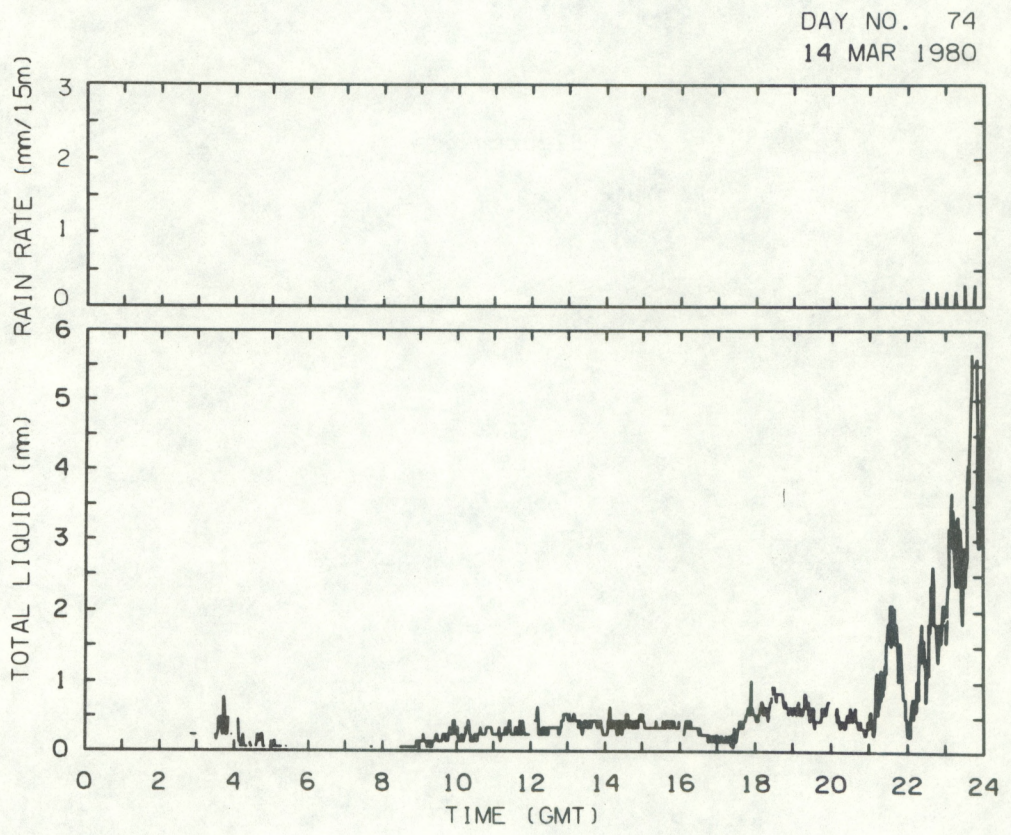
DAY NO. 74
14 MAR 1980
RAIN RATE (mm/15m)
TOTAL LIQUID (mm)
TIME (GMT)

Figure 27

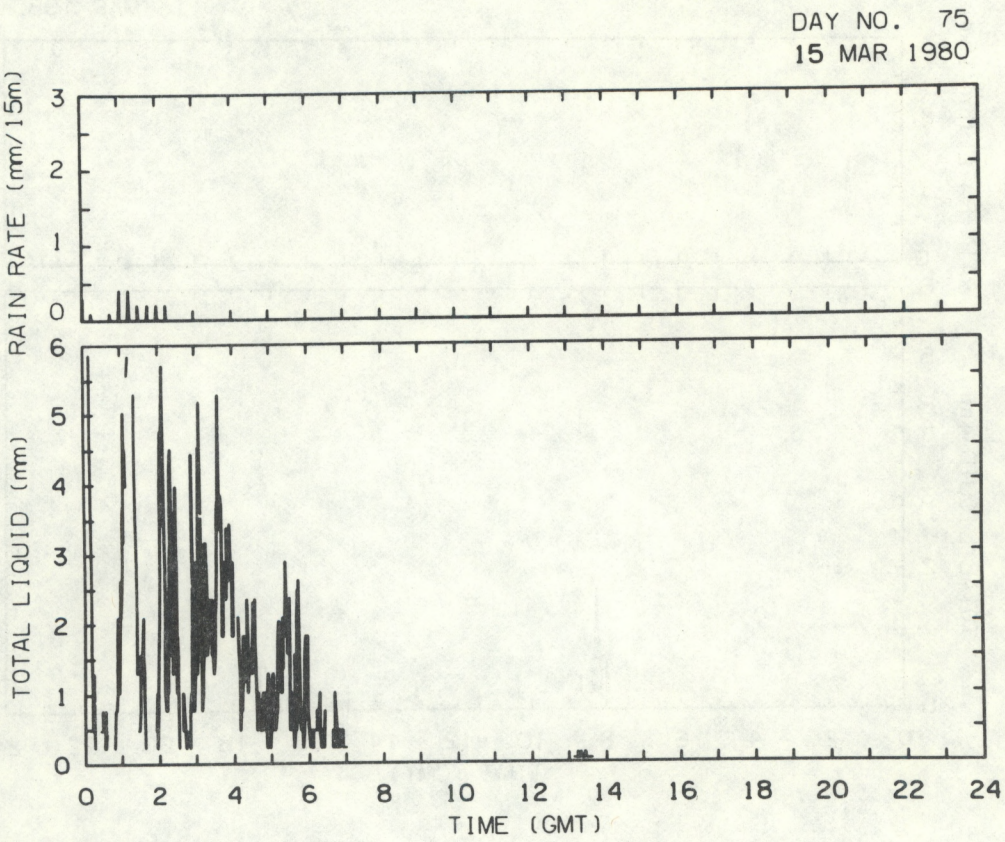
DAY NO. 75
15 MAR 1980
RAIN RATE (mm/15m)
TOTAL LIQUID (mm)
TIME (GMT)
0
1
2
3
4
5
6
0
2
4
6
8
10
12
14
16
18
20
22
24

Figure 28